The Canadian Mineralogist
Vol. 35, pp. 425-452 (1997)

THE VARIABLE ROLE OF SLAB-DERIVED FLUIDS IN THE GENERATION OF A SUITE OF PRIMITIVE CALC-ALKALINE LAVAS FROM THE SOUTHERNMOST CASCADES, CALIFORNIA

LARS E. BORG[1]

Department of Geological Sciences, University of Texas at Austin, Austin, Texas 78712, U.S.A.

MICHAEL A. CLYNNE AND THOMAS D. BULLEN

U.S. Geological Survey, 345 Middlefield Road, Menlo Park, California 94025, U.S.A.

ABSTRACT

The compositional continuum observed in primitive calc-alkaline lavas erupted from small volcanoes across the southernmost Cascade arc is produced by the introduction of a variable proportion of slab-derived fluid into the superjacent peridotite layer of the mantle wedge. Magmas derived from fluid-rich sources are erupted primarily in the forearc and are characterized by Sr and Pb enrichment (primitive mantle-normalized Sr/P > 5.5), depletions of Ta and Nb, low incompatible-element abundances, and MORB-like Sr and Pb isotopic ratios. Magmas derived from fluid-poor sources are erupted primarily in the arc axis and behind the arc, and are characterized by weak enrichment in Sr [$1.0 < (Sr/P)_N < 1.3$], weak depletions in Ta and Nb, higher incompatible-element abundances, and OIB-like Sr, Nd, and Pb isotopic ratios. Fluxing the mantle wedge above the subducting slab with H_2O-rich fluid stabilizes amphibole and enriches the wedge peridotites in incompatible elements, particularly unradiogenic Sr and Pb. The hydrated amphibole-bearing portion of the mantle wedge is downdragged beneath the forearc, where its solidus is exceeded, yielding melts that are enriched in Sr and Pb, and depleted in Ta and Nb (reflecting both high Sr and Pb relative to Ta and Nb in the fluid, and the greater compatibility of Ta and Nb in amphibole compared to other silicate phases in the wedge). A steady decrease of the fluid-contributed geochemical signature away from the trench is produced by the progressive dehydration of the downdragged portion of the mantle wedge with depth, resulting from melt extraction and increased temperature at the slab–wedge interface. Inverse correlation between incompatible-element abundances and the size of the fluid-contributed geochemical signature is generated by melting of more depleted peridotites, rather than by significant differences in the degree of melting. High-$(Sr/P)_N$ lavas of the forearc are generated by melting of a MORB-source-like peridotite that has been fluxed with a greater proportion of slab-derived fluid, and low $(Sr/P)_N$ lavas of the arc axis are produced by melting of an OIB-source-like peridotite in the presence of a smaller proportion of slab-derived fluid. This study documents the control that a slab-derived fluid can have on incompatible element and isotopic systematics of arc magmas by 1) the addition of incompatible elements to the wedge, 2) the stabilization of hydrous phases in the wedge, and 3) the lowering of peridotite solidi.

Keywords: Cascade arc, calc-alkaline, primitive lava, slab-derived fluid, Sr enrichment, California.

SOMMAIRE

Le spectre de compositions de laves calco-alcalines primitives émises par de petits volcans de part et d'autre du secteur sud de l'arc magmatique des Cascades résulte de l'introduction, dans la péridotite du coin de manteau supérieur sus-jacent, d'une proportion variable de phase fluide issue de la plaque subductée. Les magmas formés dans un tel milieu enrichi en phase fluide sont surtout mis en place dans l'avant-arc, et sont enrichis en Sr et en Pb par rapport au manteau primitif; leur rapport des teneurs normalisées du Sr et du P dépasse 5. Par contre, ils sont appauvris en Ta et en Nb, ont de faibles teneurs en éléments incompatibles, et possèdent des rapports des isotopes de Sr et de Pb semblables à ceux des basaltes des crêtes océaniques (MORB). Les magmas qui se sont formés dans des secteurs du manteau non enrichis en phase fluide sont surtout mis en place le long de l'axe de l'arc, ou dans l'après-arc. Ils sont moins fortement enrichis en Sr [$1.0 < (Sr/P)_N < 1.3$], moins fortement appauvris en Ta et Nb, ont des teneurs plus élevées en éléments incompatibles, et possèdent des rapports des isotopes de Sr, Nd et Pb plutôt semblables à ceux de basaltes d'îles océaniques. L'apport d'une phase fluide aqueuse dans le coin du manteau supérieur situé au dessus de la zone de subduction stabilise l'amphibole et mène à un enrichissement des péridotites en éléments incompatibles, surtout le Sr et le Pb non radiogéniques. La portion hydratée de la péridotite sus-jacente, porteuse d'amphibole, se trouve elle-même subductée en dessous du secteur avant-arc, milieu dans lequel son solidus est surpassé; il s'en suit la formation d'un liquide enrichi en Sr et Pb, et appauvri en Ta et Nb, ce qui témoigne des teneurs plus élevées en Sr et en Pb de la phase fluide, par rapport à Ta et Nb, et la plus grande compatibilité de Ta et de Nb dans l'amphibole que dans d'autres phases silicatées de ce milieu. Une diminution progressive de la proportion de la phase fluide en s'éloignant de la zone de subduction vers le secteur

[1] Present address: SN4/NASA Johnson Space Center, Houston, Texas 77058, U.S.A. *E-mail address*: lborg@snmail.jsc.nasa.gov

interne témoignerait de la déshydratation progressive de la partie subductée du manteau supérieur à mesure qu'elle est enfouie, ce qui a mené à l'extraction de magma et une aumentation de la température à l'interface de la plaque subductée et du manteau sus-jacent. Une corrélation inverse entre les teneurs en éléments incompatibles et l'importance relative de la signature géochimique imposée par la phase fluide résulte plutôt de l'implication, dans la réaction de fusion partielle, de péridotites de plus en plus stériles que de différences appréciables dans le taux de fusion. Les laves à rapport $(Sr/P)_N$ élevé du secteur avant-arc se seraient formées par fusion d'une péridotite ressemblant à une source de MORB qui a été sujette à une plus forte quantité de phase fluide aqueuse libérée de la plaque subductée. Les laves à faible rapport $(Sr/P)_N$ de l'axe de l'arc sont produites par fusion d'un manteau péridotitique typique de la source des basaltes des îles océaniques, en présence d'un faible quantité de phase fluide provenant de la plaque subductée. Cette étude fait état du contrôle que peut exercer la phase fluide issue de la plaque enfouie sur la géochimie des éléments incompatibles et des isotopes des magmas d'arcs volcaniques, soit par l'addition d'éléments incompatibles à la source, soit par la stabilisation de phases hydratées dans la source, soit enfin par une chute de la température du solidus.

(Traduit par la Rédaction)

Mos-clés: arc des Cascades, lave calco-alcaline, lave primitive, phase fluide dérivée de la zone de subduction, enrichissement en Sr, Californie.

INTRODUCTION

Arc magmas are generally accepted to be melts derived from compositionally varied mantle material (*e.g.*, Gill 1984, Hawkesworth *et al.* 1991) to which one or more additional components are added. Possible added components include continental crust (*e.g.*, Davidson *et al.* 1987, Hildreth & Moorbath 1988), subducted sediment (*e.g.*, Ellam & Hawkesworth 1988, Kay & Kay 1988, Morris *et al.* 1990), melts derived from a subducted slab (oceanic crust) (*e.g.*, Yogodzinski *et al.* 1994), and slab-derived fluids (*e.g.*, Ellam & Hawkesworth 1988, Tatsumi 1989, Stolper & Newman 1994). The addition of these components is deemed responsible for the high ratios of large-ion lithophile to high field-strength elements (*LILE/HFSE*), *LILE*/light-rare earths (*LREE*), and $^{207}Pb/^{204}Pb$ observed in many arc lavas, and thus for the production of the arc geochemical signature. Nevertheless, it has proved a difficult task to identify and quantify which of these potential additives are responsible in the Cascade arc.

High abundances of *LILE* and *LREE* and low abundances of *HFSE* in lavas erupted in the Cascade arc have been attributed to involvement of fluids transported into the mantle wedge from the subducting slab (Bacon 1990, Leeman *et al.* 1990, Hughes 1990, Baker *et al.* 1994). Hughes (1990) and Leeman *et al.* (1990), however, suggested that the geochemical effects of contributions from slab-derived fluid, as well as from subducted sediment, are minimal and secondary to the effects resulting from variable degrees of partial melting of MORB- and OIB-source mantle (MORB: mid-ocean ridge basalt; OIB: ocean-island basalt) in the southwestern Washington and central Oregon segments of the Cascade arc. This interpretation stems in part from the paucity of high *LILE/HFSE* basalts observed in these regions. Although primitive lavas depleted in *HFSE* are not abundant in the southernmost Cascades, they appear to be more common than in other segments of the arc, and represent an important end-member in the compositional continuum observed there. In fact, the southernmost Cascades appears to have the largest compositional diversity of primitive lavas in the Cascade arc. Thus, the southernmost Cascades is well suited for an investigation of the role of the subduction component in the petrogenesis of arc magmas.

We constrain potential sources of the high *LILE/HFSE* component (*e.g.*, crust, sediment, slab-derived melt, and slab-derived fluid) observed in primitive lavas erupted from small volcanoes across the Lassen region of California using their spatial distribution, abundances of major and trace elements, and radiogenic isotopic compositions. We begin by evaluating the role

FIG. 1. a. Tectonic setting of the Cascade range. Lavas of the High Cascades are shown in a stippled pattern; modified after McBirney (1968). Letters refer to major composite volcanoes and centers: LVC, Lassen Volcanic Center; MS, Mount Shasta; MLV, Medicine Lake Volcano, MMc, Mount McLoughlin; CLV, Crater Lake Volcano; NV, Newberry Volcano; TS, Three Sisters; MJ, Mount Jefferson; MH, Mount Hood; SVF, Simcoe Volcanic Field; MSH, Mount Saint Helens; MA, Mount Adams; MR, Mount Rainier; GP, Glacier Peak; MB, Mount Baker; MG, Mount Garibaldi; MC, Mount Cayley; MM; Meager Mountain. Study area represented by inset. b. Geographic map of study area showing location of major volcanic centers and exposure of basement rocks. Contours of upper surface of currently subducting slab from Guffanti *et al.* (1990). YVC, Yana Volcanic Center; DVC, Dittmar Volcanic Center; MVC, Maidu Volcanic Center; MV, Magee Volcano; BM, Burney Mountain; SdV, Skedaddle Volcano; SsV, Snowstorm Volcano. c. Sample-locality map. Circles are lavas with $(Sr/P)_N > 3.3$, squares are lavas with $(Sr/P)_N < 3.3$, and diamonds are lavas with undetermined Sr. $(Sr/P)_N$ is indicative of the presence of a slab-derived fluid component in the source region (see text for details). Filled symbols are primitive lavas (>6.0% MgO, >100 ppm Ni, and >200 ppm Cr). Detailed sample-locations in Borg (1995) and Clynne (1993). Note the relative abundance of high-$(Sr/P)_N$ lavas in the forearc, and of low-$(Sr/P)_N$ lavas in the arc axis and back arc.

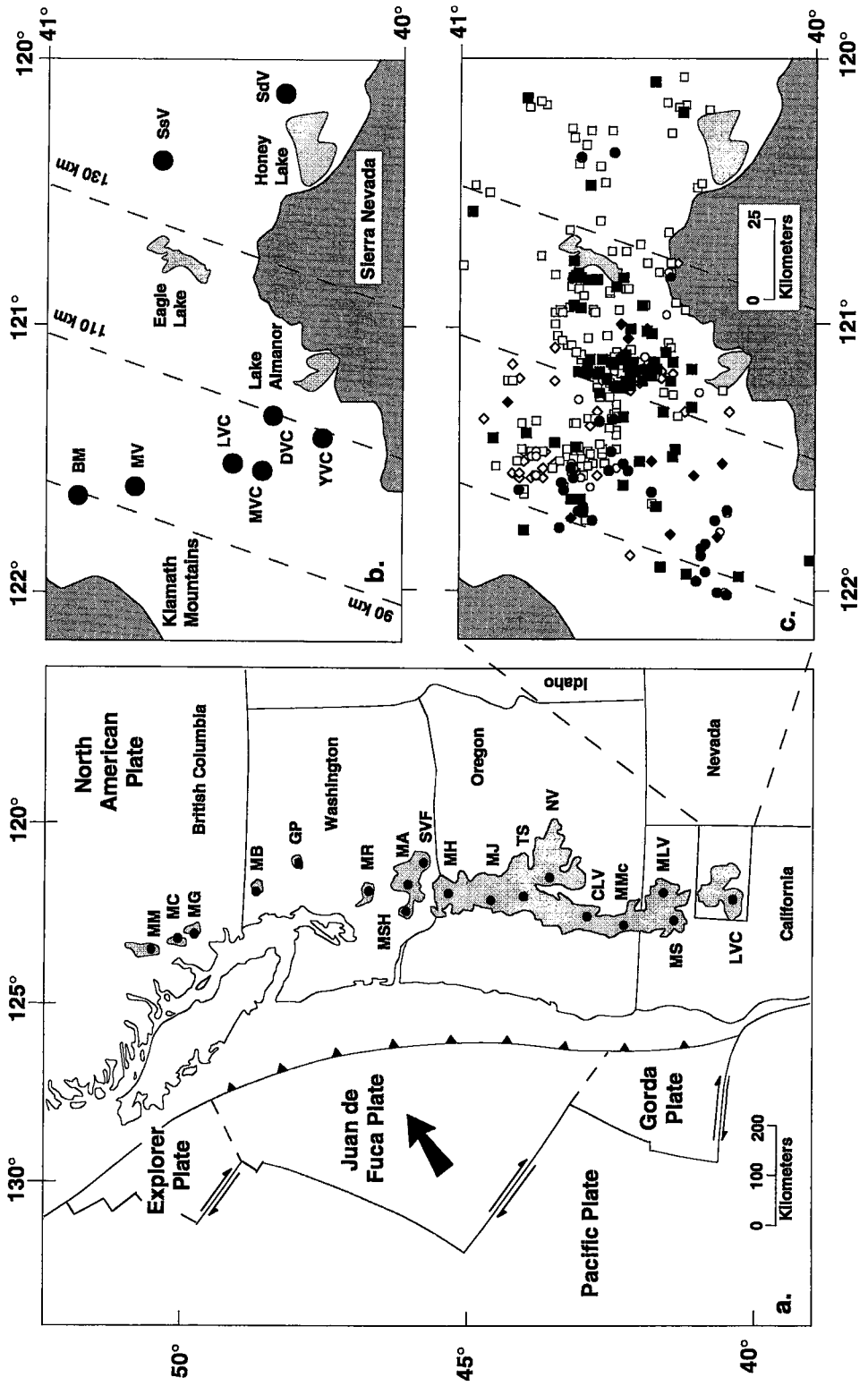
North American Plate
British Columbia
Washington
Oregon
Idaho
Nevada
California
Juan de Fuca Plate
Explorer Plate
Gorda Plate
Pacific Plate
MM
MC
MG
MB
GP
MR
MA
SVF
MH
MJ
TS
NV
CLV
MMc
MLV
MS
LVC
MSH
0 100 200 Kilometers
a.
Klamath Mountains
Sierra Nevada
Honey Lake
SdV
SsV
Eagle Lake
Lake Almanor
LVC
DVC
YVC
MVC
MV
BM
130 km
110 km
90 km
b.
0 25 Kilometers
c.
120°
125°
130°
50°
45°
40°
41°
121°
122°

TABLE 1. REPRESENTATIVE COMPOSITIONS OF LASSEN REGION LAVAS

Sample	LB91-125	LC83-347	LM87-1384	LB91-146	LC88-1329	LB91-102	LB91-105	LM88-1619	LC88-1314	LC82-886	LM92-2443	LB91-101	LC85-671	LC82-905	LC87-1190	LC86-834
Vent	Horn Mtn.	UND	UND	Ice cave chain	S. Caribou	Peak 6456	Clover Bt.	UND	Soap Bt.	UND	Cold Creek Bt.	Swain Peal Mtn.	Peal 1919	UND	Dike	Peak 2088?
Dist. (km)	376	311	324	339	328	332	335	326	281	330	305	332	321	326	304	323
Age (Ma)		0.07		0.07	0.07	0.43	0.43	0.01	1.37	0.43	0.01	0.43	0.43			0.43
$(Sr/P)_N$	1.02	1.24	1.35	1.40	1.42	1.43	1.49	1.50	1.52	1.54	1.55	1.65	1.67	1.69	1.92	1.92
SiO_2 (wt.%)	50.77	51.22	49.64	50.05	50.12	50.71	52.09	51.85	50.82	52.28	51.20	51.48	51.35	50.37	50.98	49.37
TiO_2	1.52	1.69	1.32	1.27	1.73	1.56	0.92	1.36	1.38	1.01	1.13	1.14	1.19	0.99	0.85	0.92
Al_2O_3	17.03	17.88	15.56	17.95	16.20	16.97	16.83	16.15	16.41	17.13	17.30	18.03	17.02	17.73	16.36	16.59
Fe_2O_3	2.09	1.72	1.84	1.94	2.06	1.88	1.69	1.85	1.95	1.82	1.86	1.76	1.88	1.87	1.84	1.96
FeO	7.51	6.21	6.63	7.00	7.42	6.76	6.09	6.68	7.03	6.56	6.68	6.34	6.76	6.74	6.61	7.05
FeO*	9.39	7.76	8.28	8.75	9.27	8.44	7.61	8.35	8.79	8.20	8.36	7.93	8.45	8.43	8.26	8.81
MnO	0.17	0.13	0.15	0.15	0.14	0.15	0.14	0.14	0.15	0.14	0.16	0.14	0.15	0.16	0.14	0.16
MgO	6.54	6.83	10.67	7.72	7.24	8.81	8.91	7.86	8.43	7.79	8.15	7.22	8.05	8.43	9.11	10.46
CaO	9.11	8.27	9.78	9.15	9.14	7.82	8.85	8.87	8.77	8.73	8.97	9.13	9.14	9.79	10.14	10.06
Na_2O	3.38	4.07	3.03	3.65	3.94	3.61	3.07	3.56	3.56	3.24	3.38	3.44	3.14	3.02	2.92	2.68
K_2O	1.21	1.48	0.92	0.76	1.43	1.32	1.11	1.23	1.12	1.01	0.85	0.97	1.02	0.65	0.76	0.53
P_2O_5	0.67	0.50	0.46	0.35	0.58	0.42	0.31	0.45	0.38	0.29	0.32	0.35	0.30	0.25	0.29	0.22
LOI	0.40	0.01	0.21	0.01	0.01	0.29	0.14	0.01	0.01	0.14	0.07	0.01	0.34	0.43	0.08	0.03
An. Total	99.50	98.97	99.48	100.48	100.61	99.97	99.93	100.86	100.37	99.82	99.76	99.97	99.81	99.54	100.24	99.44
Mg#	60.8	66.2	74.2	66.3	63.5	69.9	72.3	67.7	68.1	67.9	68.5	67.0	68.0	69.0	71.1	72.6
Rb (ppm)	17	24.5	24.2	19	30	24	18	28	25	15	12	14	16.8	7.3	13	14.6
Ba	830	429	408	278	526	393	323	498	448	391	410	398	371	285	320	262
Zr	198	189	148	139	176	167	134	141	172	120	138	135	130	116	100	100
Sr	660	604	601	478	796	587	452	654	559	432	482	564	487	408	540	409
Y	34	24	26	27	23	23	21	24	27	20	23	18	22	23		19
Nb	11	26	12	10	19	19	14	10	10	4	9	11	10	10		6
Ni	113	107	242	133	110	191	190	119	143	148	135	145	172	149	150	203
Cr	190	192	451	220	195	260	370	219	283	358	308	170	317	340	260	397
Co	32		32	40	36	35	39			37.9	38.6	34	36.7	41	41.1	42
Cs	0.20			0.36	0.2	0.5	0.8	0.6		0.7	0.30	0.5	0.47	0.37	0.39	0.5
Hf	4.0	3.86		3.10	3.3	3.8	3.0	2.7		2.8	2.60	3.2	2.7	2.43	2.21	2.0
Ta	0.5	1.83		0.69	0.3	1.2	1.0	0.5		0.57	0.61	0.5	0.63	0.51	0.45	0.36
Th	1.4	2.42		2.34	0.8	3.2	2.3	1.6		1.56	1.50	2.2	1.93	1.74	2.1	1.5
U	0.1	0.36		0.62	0.1	0.93	0.6	0.5		0.5	0.40	0.8	0.31	0.58	0.51	0.46
Pb	4.0[d]	3.2[d]		3.9[d]	3.0[d]				3.2[d]			4.9[d]		4.3[d]		
La	25.5[c]	22.9[c]	20.8[c]	12.1[c]	30.2[c]	18.5[c]	13.9[c]	32.2[c]	13.8[c]	13.8[c]	13.8[c]	18.2[c]	13.9[c]	12.37[d]	14.8[c]	11.4[c]
Ce	58	45.9	49.6	30	61.6	40	30	42	42.6	32.6	29	41	29	27.47	29.2	25
Nd	31	24	26.5	18	31	19	15	30	24.6	16	16	21	16.1	15.41	14	13
Sm	6.5	5.12	5.20	3.8	6.54	4.0	3.2	4.6	5.16	3.81	3.8	4.4	3.94	3.46	3.56	3.41
Eu	1.86	1.49	1.47	1.40	1.73	1.34	1.05	1.42	1.54	1.12	1.13	1.44	1.21	1.09	1.01	1.01
Gd		3.9	4.2					3.3	4.6	4.1	3.4			3.55		
Tb	0.9	0.6		0.7	0.71	0.7	0.6			0.49	0.43	0.6	0.63		0.48	0.53
Yb	2.65	2.23	1.50	2.33	2.10	1.84	1.84	2.40	2.13	2.12	1.80	1.80	3.07	2.32	1.60	1.8
Lu	0.38	0.36	0.23	0.28	0.28	0.26	0.24	0.36	0.34	0.33	0.27	0.28	0.30	0.34	0.25	0.31
$^{87}Sr/^{86}Sr$	0.70423[a]	0.70387[b]	0.70408[b]	0.70378[a]	0.70409[a]	0.70398[a]	0.70416[a]	0.70429[a]	0.70408[b]	0.70408[a]	0.70401[a]	0.70406[a]	0.70425[b]	0.70393[a]	0.70397[a]	0.70392[a]
$^{143}Nd/^{144}Nd$	0.512702	0.512819	0.512828	0.512884	0.512810	0.512830	0.512771	0.512763	0.512826	0.512791	0.512825	0.512791	0.512780	0.512813	0.512813	0.512866
$^{206}Pb/^{204}Pb$	19.026	18.915	18.835	18.945		18.960	18.988	18.963	18.907	19.002		18.979	18.965	18.972	18.937	18.997
$^{207}Pb/^{204}Pb$	15.677	15.603	15.599	15.636		15.640	15.635	15.600	15.608	15.634		15.644	15.630	15.607	15.596	15.636
$^{208}Pb/^{204}Pb$	38.782	38.572	38.512	38.672		38.707	38.690	38.596	38.571	38.703		38.723	38.637	38.612	38.568	38.704
$\delta^{18}O$	6.7	6.3	6.9	6.4	7.0	6.7	6.1	6.7	7.2	6.2	6.5	6.7	7.4	5.9		

Dist. = Distance from trench. UND = Unidentified vent. a = Isotopic analyses at University of Texas, b = Isotopic analyses at U.S.G.S., c = INAA, d = Isotope Dilution.

of differentiation on lava composition. Next, trace-element and isotope-based melting models are used to assess and quantify the effects that the addition of slab-derived components to the mantle wedge will have on melt compositions. We find that the continuum between high *LILE/HFSE* and low *LILE/HFSE* Lassen lavas primarily reflects the variable contribution of a slab-derived fluid component to the mantle wedge. The effects of the addition of the fluid component on source mineralogy and melting processes in the mantle wedge are then evaluated. Finally, we present a petrogenetic model for magma genesis in the southernmost Cascades.

TABLE 1 CONTINUED. REPRESENTATIVE COMPOSITIONS OF LASSEN REGION LAVAS

Sample	LC86-931	LC86-1006	LB92-166	LC88-1371	LB92-170	LC86-829	LB91-110	LC88-1303	LB92-168	LC87-1056	LC83-255	LB92-167	LC88-1310	LC88-1308	LC83-276	LC86-1009
Vent	Peak 8083	UND	UND	UND	UND	Peak 1791	Peak 5383	UND	CP. west M.M.	Inskip Hill	Red Mtn.	H.H. Bt.	UND	UND	CP. west P.P.	PK. 5079
Dist. (km)	322	283	285	312	283	317	350	301	287	287	301	288	280	280	310	276
Age (Ma)	0.07	1.37		1.37		1.37				0.07	0.07				0.07	1.37
$(Sr/P)_N$	2.09	2.40	2.88	3.21	3.27	3.89	4.43	4.80	4.92	5.10	5.47	5.81	5.88	5.96	6.10	6.52
SiO_2 (wt.%)	52.07	54.40	51.09	51.99	50.53	51.50	50.12	57.61	53.45	50.57	54.49	53.09	56.14	51.46	54.23	58.17
TiO_2	0.84	0.51	0.57	0.82	0.64	0.71	0.75	0.53	0.61	0.81	0.85	0.65	0.49	0.60	0.51	0.52
Al_2O_3	16.79	16.57	16.36	16.57	16.78	17.24	16.50	14.61	16.84	17.39	17.07	16.26	14.14	16.82	17.74	16.00
Fe_2O_3	1.65	1.55	1.68	1.86	1.78	1.63	1.98	1.53	1.67	1.71	1.40	1.62	1.48	1.64	1.43	1.25
FeO	5.92	5.56	6.03	6.68	6.40	5.87	7.14	5.51	6.00	6.14	5.05	5.82	5.34	5.90	5.15	4.50
FeO*	7.40	6.95	7.54	8.35	7.99	7.33	8.92	6.88	7.50	7.67	6.31	7.28	6.67	7.38	6.43	5.62
MnO	0.13	0.14	0.14	0.15	0.15	0.13	0.12	0.12	0.14	0.15	0.10	0.14	0.12	0.16	0.11	0.10
MgO	8.85	8.33	11.06	8.34	10.52	9.20	8.86	7.49	7.65	8.24	7.73	8.15	10.20	9.09	6.87	7.57
CaO	9.62	8.86	10.07	10.28	9.89	10.42	10.77	8.7	9.81	12.09	8.98	11.15	8.52	11.25	10.38	7.72
Na_2O	3.09	3.23	2.56	2.92	3.67	2.57	2.68	2.69	2.87	2.57	3.47	2.69	2.57	2.59	2.86	3.25
K_2O	0.84	0.64	0.31	0.22	0.51	0.61	0.93	1.11	0.83	0.23	0.63	0.32	0.87	0.41	0.61	0.80
P_2O_5	0.20	0.21	0.13	0.09	0.13	0.12	0.16	0.10	0.13	0.10	0.23	0.13	0.13	0.08	0.11	0.12
LOI	0.10	0.13	0.30	0.05	0.08	0.18	0.06	1.19	0.48	0.01	0.74	0.01	0.89	0.74	0.01	0.09
An. Total	100.04	100.63	100.34	100.81	99.87	99.79	100.16	99.06	100.02	100.05	98.40	101.41	99.03	98.69	99.22	100.03
Mg#	72.7	72.7	76.6	69.2	74.6	73.7	68.9	70.8	69.5	70.5	73.2	71.4	77.3	73.3	70.4	75.0
Rb (ppm)	15	14	6	6	8.7	6.7	19	11	20	5.5	12.9	8	10.9	6.2	15	9.7
Ba	309	307	132	140	158	187	308	298	326	85	293	106	296	121	176	181
Zr	98	114	74	130	64	75	86	103	101	77	139	81	93	69	77	100
Sr	405	492	364	280	416	452	692	464	617	494	1220	732	741	462	650	758
Y	17	22	19		16	15	25	14	20	20	15	16	17	22	13	17
Nb	7	4	4			2	2	2	2	6	3	2	7	5	1	3
Ni	165	170	222	100	260	158	75	69	78	44	136	61	196	166	52	183
Cr	482	449	616	344	581	401	250	336	198	243	249	253	664	444	170	242
Co		35.2	41	40.5	42	39	41	30.5	34	34	32	38	37	38		30
Cs		0.2	0.3	0.17	0.22	0.43	0.4	1.4	0.5	0.23	0.29	0.2		0.35		0.47
Hf		2.2	1.2	1.8	1.6	1.65	1.7	2.47	2.1	1.71	2.66	1.4	1.98	1.35		1.83
Ta		0.12	0.3	0.12	0.095	0.25	0.3	0.18	0.3	0.10	0.33	0.3	0.14	0.14		0.13
Th		2.9	0.5	0.62	1.0	1.1	2.4	2.68	1.8	0.55	1.96	0.8	2.05	0.55		1.14
U		0.64	0.2	0.27	0.27	0.25	0.5	0.79	0.7	0.30	0.54	0.4	0.49			0.8
Pb										2.1[d]	4.3[d]	2.8[d]	2.1[d]	1.5[d]	2.6[d]	3.4[d]
La		17.5[c]	4.0[c]	4.9[c]	6.4[c]	7.0[c]	12.0[c]	9.78[c]	10.0[c]		18.6[c]	7.3[c]	10.6[c]		6.2[c]	7.53[d]
Ce		33.3	10	12	12	15	23	20	23		37.8	15.0	22.6		12.9	16.04
Nd		16	6	8.2	8.0	8.6	14	10	11		21	8	11.8		7.6	9.32
Sm		3.61	1.5	2.59	2.18	2.47	3.3	2.73	2.5		3.77	1.8	2.76		2.00	2.12
Eu		1.00	0.52	0.88	0.73	0.80	1.07	0.75	0.85		1.09	0.62	0.78		0.63	0.73
Gd											3.2				1.7	2.01
Tb		0.43	0.3	0.53	0.38	0.44	0.5	0.44	0.4		0.42	0.3	0.31		0.27	
Yb		1.60	1.32	2.60	1.40	1.60	1.60	1.50	1.25		1.30	1.11	1.17		1.10	0.98
Lu		0.24	0.19	0.39	0.21	0.22	0.23	0.24	0.20		0.22	0.16	0.18		0.21	0.16
$^{87}Sr/^{86}Sr$	0.70401[a]	0.70412[a]	0.70385[a]	0.70367[a]	0.70343[a]	0.70401[a]	0.70349[a]	0.70326[a]	0.70341[a]	0.70318[b]	0.70308[b]	0.70296[a]	0.70292[b]	0.70321[b]	0.70345[b]	0.70305[b]
$^{143}Nd/^{144}Nd$	0.512816	0.512773	0.512905	19.039	0.512918	0.512799	0.512891	0.512875	0.512829	0.512934	0.512901	0.512969	0.512913	0.512961	0.512850	0.512869
$^{206}Pb/^{204}Pb$	19.067		18.892	15.643	18.809	18.975	18.881		18.873	18.902	18.932	18.778	18.735	18.757	18.811	18.674
$^{207}Pb/^{204}Pb$	15.648		15.606	38.727	15.590	15.613	15.600		15.600	15.591	15.617	15.577	15.545	15.547	15.553	15.535
$^{208}Pb/^{204}Pb$	38.787		38.534	0.512991	38.419	38.567	38.509		38.501	38.466	38.562	38.332	38.242	38.272	38.323	38.217
$\delta^{18}O$		6.7	6.6	5.7	6.5		6.2	7.0	6.6	6.4	6.9	6.2	7.4	7.2	6.5	6.9

Dist. = Distance from trench. CP = cinder pit. M.M. is Magee Mtn., H.H. is Horse Haven Butte, P.P. is Prospect Peak, and UND is Unidentified vent. a = Isotopic analyses at University of Texas, b = Isotopic analyses at U.S.G.S., c = INAA, d = Isotope Dilution.

GEOLOGY OF THE LASSEN REGION

The study area is the southernmost segment of the Cascade arc as defined by Guffanti & Weaver (1988), and is located in northeastern California (Fig. 1a). It is designated here as the Lassen region. The field area contains a chain of Pliocene to Holocene volcanoes that includes the Lassen, Maidu, Yana, and Dittmar volcanic centers, Magee Volcano, and Burney Mountain (Fig. 1b). The area extends eastward to a near-linear belt of Miocene stratocones that parallels the modern arc and includes Skedaddle and Snowstorm volcanoes (Fig. 1b).

The Lassen region is underlain by Phanerozoic igneous and metamorphic rocks of the Klamath and Sierra Nevada provinces, which crop out to the northwest and south, respectively. To the southwest, sediments of the Great Valley crop out; to the east lies the Basin and Range province. The presence of northwest-trending normal faults indicates impingement of the Basin and Range extensional tectonic regime on the region. Chains of cinder cones and shield volcanoes were erupted along faults that are parallel to modern faults of the Basin and Range, indicating that faulting and volcanism have been contemporaneous (Guffanti *et al.* 1990).

The Lassen region contains numerous calc-alkaline mafic lavas erupted from monogenetic cinder volcanoes and small shield volcanoes that are the focus of this investigation. These volcanoes were active for short periods of time (generally less than 1000 yr; Guffanti *et al.* 1990) and produced relatively few (approximately one to five) lava flows. Guffanti *et al.* (1990) identified 537 vents in the region and assigned ages to them using radiometric dating techniques, paleomagnetic studies and field observations. They observed that the volcanic centers became progressively younger to the west, reflecting a westward shift in volcanism since about 12 Ma. Despite the small sizes of individual cinder-cone and shield volcanoes (1–5 km^3), this type of volcanism is representative of volcanic processes in the region because it has produced a large percentage of the total erupted material observed in the southernmost Cascades (Sherrod & Smith 1990). Lavas erupted from small volcanoes in the Lassen region form an excellent basis for the study of arc petrogenesis because they are more primitive than lavas erupted from large complex centers in the region (Borg 1995), and are geographically more extensive.

Analytical methods

Major-element analyses have been obtained on over 400 samples of lava, granitic and metasedimentary country-rocks by wavelength-dispersion X-ray fluorescence (XRF) techniques at the U.S. Geological Survey at Lakewood, Colorado. The focus of this study is 140 lavas that have greater than 6.0 wt.% MgO and represent the most primitive compositions observed in the region. A representative group of these lavas is presented in Table 1. Additional whole-rock compositions are presented by Clynne (1993), Borg (1995), and Bacon *et al.* (1997). Major elements, expressed as oxides, are normalized to 100% anhydrous after Fe_2O_3 was set equal to 0.2 times the total iron (expressed as Fe_2O_3), and are therefore directly comparable to data from the Lassen Volcanic Center published by Bullen & Clynne (1990). Original analytical totals are shown to demonstrate the quality of the analyses. KEVEX (energy-dispersion XRF) analysis for Rb, Ba, Zr, Sr, Y, Nb, Ni, and Cr has been completed on 98 samples of primitive lava at the U.S. Geological Survey in Menlo Park, California. Analytical uncertainties for the XRF data (with the exception of Rb and Sr, which are significantly better; see Clynne 1993) are similar to those reported in Bacon & Druitt (1988). Concentrations of the remaining trace elements were determined by instrumental neutron-activation analysis (INAA) at Reston, Virginia (techniques reported in Baedecker & McKown 1987). Pb concentrations were determined by isotope dilution at the University of Texas and the U.S. Geological Survey. Isotope dilution data are accurate to approximately 1%.

Whole-rock isotopic analyses of Sr, Nd, and Pb were determined on 41 samples of lava, granitic, and metasedimentary country-rock using a multi-collector Finnigan MAT 261 mass spectrometer at the University of Texas at Austin. Pb samples were leached for fifteen minutes in warm 2N HCl prior to digestion in HF. Total Sr, Nd, and Pb procedural blanks averaged 70, 25, and 65 pg, respectively. Approximately 500 ng of Sr and Nd, and 150 ng Pb were routinely loaded for mass spectrometer runs. Sr and Nd isotopic ratios were normalized with an exponential mass-fractionation law using $^{86}Sr/^{88}Sr = 0.1194$ and $^{146}Nd/^{144}Nd = 0.7219$. The average $^{87}Sr/^{86}Sr$ value ($\pm$ one standard deviation) from thirty-one measurements of NBS–987 Sr standard completed during the course of the investigation is 0.710253 ± 13. Twenty measurements of $^{143}Nd/^{144}Nd$ for the Caltech nNd Beta standard average 0.511898 ± 5 ($\varepsilon_{Nd} = -14.43 \pm 0.10$), and five measurements of $^{143}Nd/^{144}Nd$ for the LaJolla Nd standard averaged 0.511850 ± 5 ($\varepsilon_{Nd} = -15.37 \pm 0.10$). Accuracy of Sr and Nd isotopic ratios is estimated to be ± 0.00002 and ± 0.000018 on the basis of replicate analyses of samples and rock standards. Pb isotopic ratios were corrected for 0.11% fractionation per atomic mass unit (*amu*) based upon 33 concurrent analyses of the NBS–981 Pb standard. Precision of Pb analyses is estimated to be 0.02% per *amu* based upon replicate analyses of the NBS–981 standard and lava LC82–905. An additional 27 Sr, Nd, and Pb, and 44 oxygen analyses were completed at the U.S. Geological Survey in Menlo Park, California. Analytical procedures are described in Bullen & Clynne (1990).

Petrography

Lavas selected for geochemical analysis range from primitive basalts and Mg-andesites to somewhat evolved basaltic andesites. The most primitive lavas are sparsely porphyritic (~5% phenocrysts) and have simple mineral assemblages consisting of olivine or olivine + spinel. Some lavas also contain chromian diopside. Small phenocrysts of olivine are unzoned and have compositions that range from Fo_{90} to Fo_{86}, with CaO content that indicates crystallization around 1225 to 1250°C (Clynne & Borg 1997). The less primitive lavas can be more crystal-rich and contain a combination of olivine, clinopyroxene, and calcic plagioclase.

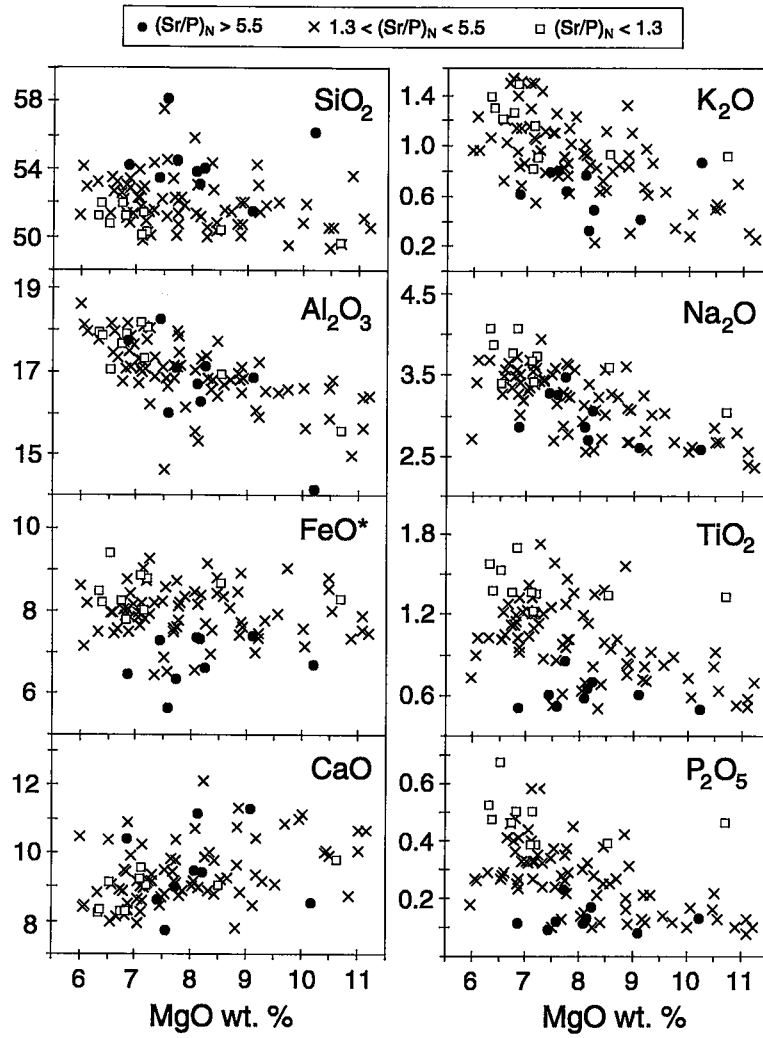

FIG. 2. MgO variation diagrams of primitive Lassen lavas. Solid circles depict strongly spiked lavas, with $(Sr/P)_N > 5.5$, and open squares represent weakly spiked lavas, with $(Sr/P)_N < 1.3$. Crosses are lavas with $1.3 < (Sr/P)_N < 5.5$. The strongly spiked lavas are depleted in Ti, Fe, Na, K, and P, and enriched in Si relative to the weakly spiked lavas at equivalent MgO. Lavas from both groups have similar Ca contents.

The phenocryst compositions reported for the primitive lavas in the Lassen region by Clynne & Borg (1997) are similar to compositions reported from primitive lavas in many arcs *e.g.*, Japan (Tatsumi & Ishizaka 1982), the Aleutian arc (Kay & Kay 1985), the Kurile arc (Bailey *et al.* 1989), and the Mexican volcanic belt (Luhr & Carmichael 1985). Furthermore, the compositions of the mafic minerals are similar to, or approach, compositions found in many bodies or nodules of ultramafic rock (Dick & Fisher 1984). Thus, the compositions of mafic phenocrysts present in the primitive calc-alkaline lavas of the Lassen region are sufficiently magnesian and compatible-element-rich to be in equilibrium with peridotites.

Geochemistry of lavas

The lavas erupted from monogenetic cinder cones and small shield volcanoes consist of calc-alkaline low- to high-K basalt through dacite, according to the criteria of Irvine & Baragar (1971), Miyashiro (1974), and Gill (1981). Sample localities and representative whole-rock

compositions are presented in Figure 1c and Table 1 [more detailed sample localities and additional results of whole-rock analyses are presented in Clynne (1993) and Borg (1995)]. A group of remarkably homogeneous tholeiitic lavas, characterized by <0.3 wt.% K_2O, $0.9 < FeO^*/MgO < 1.2$, and $48 < SiO_2 < 50$ wt.%, are also present and coeval with calc-alkaline magmatism in the Lassen region (Bacon *et al.* 1997). These lavas are not considered here because 1) their spatial, compositional and, therefore, probable petrogenetic affinities are to Basin and Range lavas (Bullen & Clynne 1989, Guffanti *et al.* 1990, Clynne 1993), and 2) the limited constraints they are likely to place on the sources of the arc geochemical signature.

Calc-alkaline lavas in the Lassen region exhibit highly variable compositions (Fig. 2). MgO contents in sparsely to moderately porphyritic lavas range from 4.4 to 11.2 wt.% in basalts, 3.9 to 10.9 wt.% in basaltic andesites, 1.6 to 7.6 wt.% in andesites, and 1.8 to 3.2 wt.% in dacites. In addition, trace-element abundances are highly varied [Ba ranges from 85 to 954 ppm, Rb ranges from 2 to 38 ppm, and Cr ranges from 39 to 616 ppm in lavas with MgO > 6.0; Table 1; Clynne (1993, unpubl. data), Borg (1995)]. Primitive lavas are defined as having moderately high levels of compatible elements (MgO > 6%, Ni > 100 ppm, and Cr > 200 ppm) for the purpose of this paper. Note that some lavas with relatively high MgO contents (7–10 wt.%) have high SiO_2 (54–58 wt.%) as well (Fig. 2). The relative primitiveness of these lavas is illustrated by the presence of spinel phenocrysts, their sparsely phyric nature, and the high Mg# [= molar 100 Mg/(Mg + Fe^{2+})] of their silicate phases (average Mg# from results of 36 electron-microprobe analyses of olivine is 86.1; Clynne & Borg 1997). Thus, as suggested by Borg *et al.* (1992, 1994) and Clynne (1993), basalts, basaltic andesites, and andesites all have primitive representatives.

The calc-alkaline lavas of the Lassen region display a compositional and isotopic continuum. The ends of the continuum can be numerically defined by the degree that Sr is enriched in the lavas over other similarly incompatible elements. This definition has petrogenetic significance because most geochemical and isotopic characteristics of the lavas correlate with Sr enrichment (see below). The Sr enrichment is hereafter called a Sr spike, and is defined as normalized $(Sr/P)_N > 1$ [*N* refers to normalization to values of primitive mantle as defined by Sun & McDonough (1989)]. Good correlation between $(Sr/P)_N$ and $(Sr/LREE)_N$ demonstrates that these ratios are analogous, although $(Sr/P)_N$ is used because more data are available for P than for the *LREE*. It is important to note that the variations in Sr/P and Sr/*LREE* observed in the lavas are not simply the result of depletions in P and *LREE* abundances, but instead the result of simultaneous increase in the abundance of Sr and accompanying depletion in most incompatible elements (including P and *LREE*).

There is a continuous range of $(Sr/P)_N$ in primitive Lassen lavas from 1.0 to 6.7 (Table 1). For convenience, we define one end of the continuum as the average of lavas with the smallest spike [$(Sr/P)_N < 1.3$], whereas the other end is defined as the average of lavas with the largest spike [$(Sr/P)_N > 5.5$; Table 2]. These averages are hereafter referred to as weakly and strongly spiked compositional end-members, respectively. Using average values to represent the ends of the continuum alleviates inaccuracies resulting from basing petrogenetic models on only one or two of the most disparate compositions observed in over 100 analyzed lavas. Furthermore, the most disparate lavas have compositions that are similar to the average of the strongly and weakly spiked end-members. Therefore, except for the uncertainties associated with sampling, the results

TABLE 2. AVERAGE COMPOSITIONS OF END-MEMBERS

	Strongly spiked end-member $(Sr/P)_N > 5.5$ (average = 6.1)		Weakly spiked end-member $(Sr/P)_N < 1.3$ (average = 1.2)		Confidence Interval (t-Test)
SiO_2 (wt.%)	54.3 ±1.9	(9)	50.9 ±0.8	(10)	99.9
TiO_2	0.61 ±0.11	(9)	1.41 ±0.14	(10)	99.9
Al_2O_3	16.7 ±1.2	(9)	17.4 ±0.8	(10)	90
FeO*	6.77 ±0.60	(9)	8.45 ±0.47	(10)	99.9
MnO	0.12 ±0.02	(9)	0.15 ±0.01	(10)	99.9
MgO	8.15 ±0.99	(9)	7.35 ±1.23	(10)	80
CaO	9.49 ±1.21	(9)	8.88 ±0.57	(10)	80
Na_2O	2.96 ±0.32	(9)	3.65 ±0.32	(10)	99.9
K_2O	0.63 ±0.19	(9)	1.14 ±0.23	(10)	99.9
P_2O_5	0.13 ±0.05	(9)	0.47 ±0.09	(10)	99.9
Mg#	72.7 ±2.4	(9)	65.6 ±3.7	(10)	99.9
Ni (ppm)	129 ±47	(9)	134 ±43	(9)	<50
Cr	258 ±120	(9)	275 ±123	(5)	<50
Cs	0.32 ±0.14	(3)	0.44 ±0.16	(2)	<50
Rb	14.3 ±5	(9)	21 ±5	(10)	90
Ba	217 ±74	(9)	463 ±210	(5)	90
Th	1.30 ±0.60	(9)	2.05 ±0.57	(3)	90
U	0.58 ±0.20	(8)	0.49 ±0.18	(2)	<50
Nb	3.4 ±1.9	(8)	16 ±6	(10)	99.5
Ta	0.26 ±0.09	(3)	1.01 ±.72	(3)	60
Pb	2.78 ±0.99	(9)	3.55 ±0.44	(3)	99
Sr	649 ±241	(9)	536 ±61	(10)	90
Zr	94 ±21	(9)	164 ±29	(10)	99.9
Hf	1.96 ±0.38	(3)	3.65 ±0.48	(3)	99.5
Y	16.4 ±3	(9)	25 ±5	(10)	99.5
La	9.56 ±5.66	(5)	20.3 ±5.8	(4)	97.5
Ce	20.2 ±10.9	(5)	45.9 ±11.7	(4)	97.5
Nd	11.4 ±5.8	(5)	24.9 ±5.4	(4)	99
Sm	2.40 ±0.83	(5)	5.16 ±1.10	(4)	99.5
Eu	0.78 ±0.18	(5)	1.56 ±0.21	(4)	99.9
Gd	2.43 ±0.56	(4)	4.05 ±0.21	(3)	99.5
Tb	0.36 ±0.08	(2)	0.73 ±0.15	(3)	99.5
Dy	2.22 ±0.49	(3)	3.27	(1)	—
Er	1.48 ±0.59	(2)	1.71	(1)	—
Yb	1.29 ±0.37	(5)	2.18 ±0.49	(4)	97.5
Lu	0.21 ±0.06	(5)	0.31 ±0.07	(4)	90
$^{87}Sr/^{86}Sr$	0.70311 ±19	(6)	0.70398 ±16	(6)	99.9
$^{143}Nd/^{144}Nd$	0.51291 ±5	(6)	0.51281 ±6	(6)	99.9
$^{206}Pb/^{204}Pb$	18.77 ±6	(6)	18.95 ±7	(6)	99.9
$^{207}Pb/^{204}Pb$	15.56 ±2	(6)	15.65 ±4	(6)	99.9
$^{208}Pb/^{204}Pb$	38.31 ±7	(6)	38.70 ±13	(6)	99.9
$\delta^{18}O$	6.9 ±0.4	(6)	6.5 ±0.3	(6)	95

(n) is number of analyses. ± is 1 standard deviation.

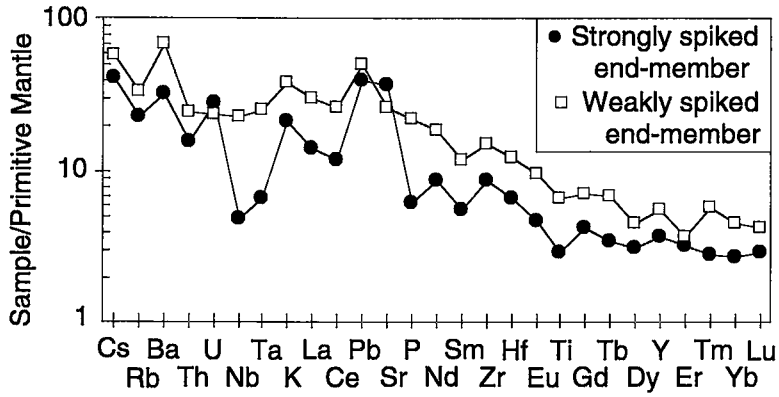

FIG. 3. Primitive-mantle-normalized spidergram of average end-member compositions presented in Table 2. Circles depict average composition of primitive lavas with $(Sr/P)_N > 5.5$, and squares are average composition of primitive lavas with $(Sr/P)_N < 1.3$. Normalization to values of Sun & McDonough (1989). Primitive mantle values are (in ppm): Cs (0.032), Rb (0.635), Ba (6.989), Th (0.085), U (0.021), Nb (0.713), Ta (0.041), K (250), La (0.687), Ce (1.775), Pb (0.0079), Sr (21.1), P (95), Nd (1.354), Sm (0.444), Zr (11.2), Hf (0.309), Eu (0.168), Ti (1300), Gd (0.596), Tb (0.108), Dy (0.737), Y (4.55), Er (0.48), Tm (0.074), Yb (0.493), Lu (0.074). Note that the strongly spiked lavas are enriched in Sr and Pb, and depleted in Nb and Ta. Also note that the strongly spiked lavas are depleted in almost all incompatible elements relative to the weakly spiked lavas.

of petrogenetic models based on these averages will not vary significantly from the results that would be based on a single bulk composition. It should be noted that the compositions of the end-members do not change significantly if only lavas with MgO > 8.0 wt.% are used to calculate the average composition. This stems from the fact that abundances and ratios of incompatible elements and isotopic ratios of the lavas are not dramatically affected by early differentiation (Borg 1995, Guffanti *et al.* 1996). Thus, we use all lavas with MgO > 6.0 wt.% because this increases the sample base significantly and places better constraints on our petrogenetic models.

Variation diagrams of the primitive lava data-set (Fig. 2) demonstrate the variable relations between major-element abundances in the lavas and the differences among lavas at the ends of the continuum. There are good inverse correlations between some major elements (such as Al, K, Na, Ti, and P) and Mg, whereas other major elements (such as Si, Fe, and Ca) do not systematically vary with Mg. Strongly spiked lavas have higher SiO_2 and lower FeO*, K_2O, Na_2O, TiO_2, and P_2O_5 than the weakly spiked lavas at equivalent MgO. The differences in major-element composition between the end-members are verified statistically by the t-test, which demonstrates that most major-element contents are different above the 99.5% confidence interval (Table 2). The incompatible-element concentrations in the weakly and strongly spiked end-members are presented in Figure 3. The weakly spiked compositional end-member is characterized by lavas with relatively smooth incompatible-element patterns on primitive-mantle-normalized spidergrams, and high abundances of incompatible elements. In contrast, the strongly spiked compositional end-member has pronounced relative enrichment in Sr and Pb, and depletion in Ta and Nb on primitive-mantle-normalized spidergrams, and relatively low concentrations of most incompatible elements.

The strongly and weakly spiked lavas are isotopically distinct as well, and have isotopic systematics that are unlike many potential mantle and crustal sources likely to be present in the Lassen region. The strongly spiked lavas are isotopically the most similar to MORB of any lavas analyzed in the region. In fact, the lavas with the largest Sr spikes have Sr and Pb isotopic ratios that are very similar to Juan de Fuca MORB (Figs. 4, 5; White *et al.* 1987, Eaby *et al.* 1984). The $^{143}Nd/^{144}Nd$ values of the same lavas, however, are significantly lower than Juan de Fuca MORB (Hegner & Tatsumoto 1987). As a result, these lavas fall to the left of the Sr–Nd mantle array (Fig. 4). In contrast, weakly spiked lavas have more radiogenic Sr and Pb isotopic ratios and lower $^{143}Nd/^{144}Nd$, and fall more toward the middle of the Sr–Nd mantle array (Figs. 4, 5). Although Sr and Nd isotopic ratios of the weakly spiked lavas are similar to ratios in some OIB, as well as to some Mesozoic crustal (granitic and metasedimentary) country-rocks in the region (Fig. 4), the $^{207}Pb/^{204}Pb$ values are commonly

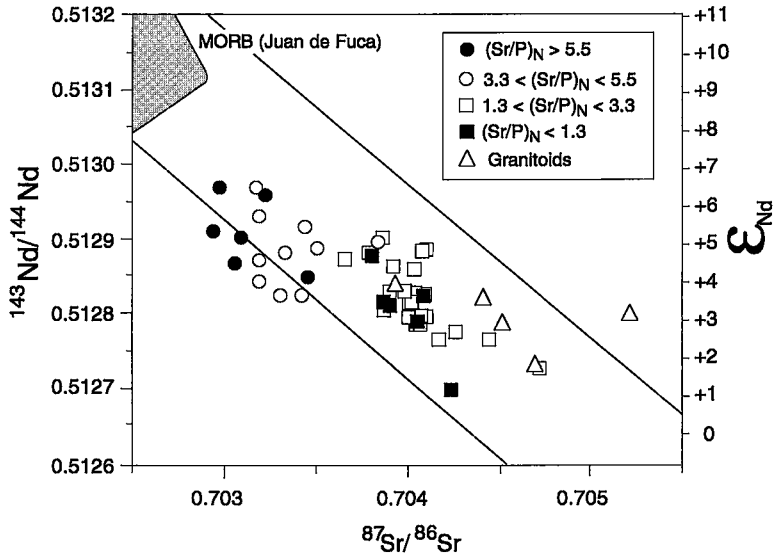

FIG. 4. Sr–Nd plot of primitive Lassen lavas and Sierran Mesozoic granitic rocks from the region. Juan de Fuca MORB field from White *et al.* (1987) and Hegner & Tatsumoto (1987). Many lavas with $(Sr/P)_N > 3.3$ have a $^{87}Sr/^{86}Sr$ value that is similar to Juan de Fuca MORB, but have a $^{143}Nd/^{144}Nd$ value that is significantly lower, and therefore fall to the left and outside of the mantle array. In contrast, lavas with $(Sr/P)_N < 3.3$ lie within the mantle array. Lavas that fall to the left of the mantle array are enriched in a high-(Sr/Nd) fluid-contributed component, whereas lavas that lie on the array lack large amounts of this component (see text).

more radiogenic than values for pristine Northern Hemisphere Reference Line (NHRL)-like OIB, Mesozoic crust, or Gorda Basin sediment (Fig. 5). It should be noted that whereas Sr, Nd, and Pb isotopic values are different in strongly and weakly spiked lavas, $\delta^{18}O$ values, although elevated with reference to typical mantle values (5.6 to 7.8‰), are not distinct (Table 1).

The $(Sr/P)_N$ value correlates with the major element, trace element, and isotopic composition of the lavas (Fig. 6). As $(Sr/P)_N$ increases, the lavas are enriched in SiO_2, more depleted in most incompatible elements, and isotopically more MORB-like. The abundance of some elements, such as Fe, steadily decreases as $(Sr/P)_N$ increases, whereas that of other elements, like Na and K, demonstrate a less linear relationship with $(Sr/P)_N$. Despite the fact that the correlation between $(Sr/P)_N$ and abundance of incompatible elements is rarely linear, the strongly spiked end-member invariably has lower abundances of incompatible elements than the weakly spiked end-member (Table 2). As $(Sr/P)_N$ increases, $(U/Ta)_N$ (Fig. 6), $(U/Nb)_N$, and $(Pb/P)_N$ (not shown) increase. Thus, the magnitude of Ta and Nb depletion and Pb enrichment (relative to other incompatible elements observed in the lavas) correlates with the extent of Sr enrichment (Fig. 6).

Spatial systematics

A key observation that strongly constrains any petrogenetic model for the southernmost Cascades is the fact that the presence of the Sr spike correlates with the location of individual samples within the arc (Fig. 7a). Figures 7a and 7b illustrate the distribution of strongly and weakly spiked lavas at different time-intervals because migration of the arc axis through time requires that the spatial distribution of the lavas within the arc be evaluated in a temporal context. It is apparent from Figure 7b that for the ≤0.07 Ma time-slice, the strongly spiked lavas are found primarily in the forearc region, whereas the weakly spiked lavas are found throughout the main arc axis and backarc regions, but are rare in the forearc. Although there are significantly fewer data, the same pattern appears to hold for the older time-slices.

PETROGENESIS OF THE SOUTHERNMOST CASCADES LAVAS

This section examines potential processes that may produce the geochemical differences between the strongly and weakly spiked lavas. We first investigate the role of differentiation, including assimilation – frac-

tional crystallization (AFC) processes, in the petrogenesis of the calc-alkaline lava suite. Then, we discuss the effects that the potential addition of slab-derived components (such as sediment, melt, and fluid) to the mantle wedge would have on the generation of the geochemical signatures of the strongly and weakly spiked lavas.

Crustal differentiation processes

Differentiation alone cannot produce all the systematic compositional variation observed in the southernmost Cascade lavas for several reasons. The geochemical differences between the strongly and weakly spiked lavas are most apparent in the most primitive lavas, which demonstrate the least evidence of differentiation. The most primitive lavas are sparsely porphyritic, have phenocrysts with a high Mg# (Clynne & Borg 1997), and have high abundances of compatible elements, indicating that they are only slightly evolved from primary magmas in equilibrium with mantle peridotite. In addition, the observed differentiation-induced trends are not parallel to compositional continua observed from the strongly to the weakly spiked lavas (Clynne 1993, Borg 1995). For example, generation of the enrichments in Sr and Pb, and depletions in Ta and Nb observed in the strongly spiked lavas, cannot be accomplished through fractional crystallization because Sr, Pb, Ta, and Nb all behave incompatibly in the plagioclase-free fractionating assemblage observed in lavas with less than 53 wt.% SiO_2 (Borg 1995).

It is also difficult to generate one end of the continuum from the other by AFC processes because these processes generally require the simultaneous increase of SiO_2, incompatible elements, and decrease of most compatible elements (Clynne 1993). Assimilation of felsic mid- to upper-level crustal rocks could account for the high SiO_2 abundances in the high $(Sr/P)_N$ lavas, but cannot produce the other geochemical differences observed between the strongly and weakly spiked lavas. Assimilation of old continental crust is not supported by

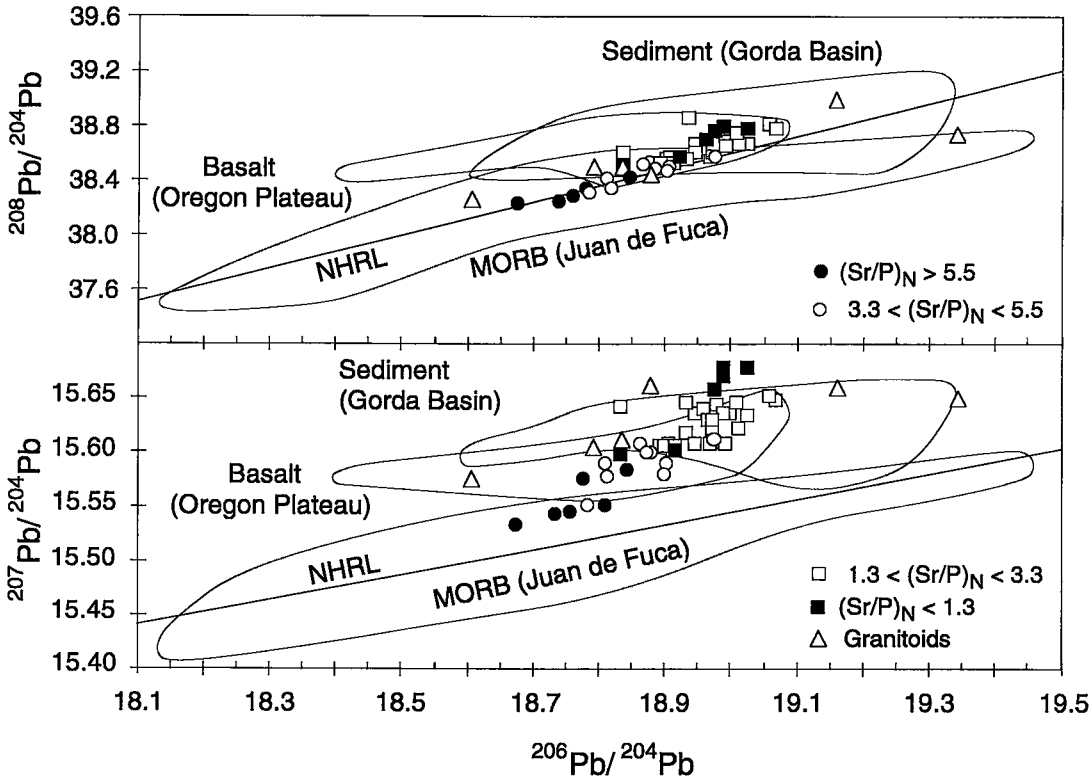

FIG. 5. Pb isotopic plot of primitive Lassen lavas and Sierran Mesozoic granitic rocks observed in the region. Symbols as in Fig. 4. Juan de Fuca MORB field from White *et al.* (1987), Hegner & Tatsumoto (1987), Church & Tatsumoto (1975). The northern hemisphere reference line (NHRL) is from Hart (1984), and is based on Pb isotopic values from MORB and OIB. The field of Oregon plateau basalts is from Carlson & Hart (1987) and Church (1985). Data on Gorda basin sediments are taken from Church (1976) and Church & Tilton (1973). Strongly spiked Lassen lavas have Pb isotopic ratios similar to those of Juan de Fuca MORB and fall near the NHRL, whereas weakly spiked lavas have $^{208}Pb/^{204}Pb$ and $^{206}Pb/^{204}Pb$ values that are similar to the sediments of the Gorda Basin. Note that $^{207}Pb/^{204}Pb$ values of many of the weakly spiked lavas are more radiogenic than the sediments of the Gorda Basin or Mesozoic granitic rocks of the Sierra Nevada.

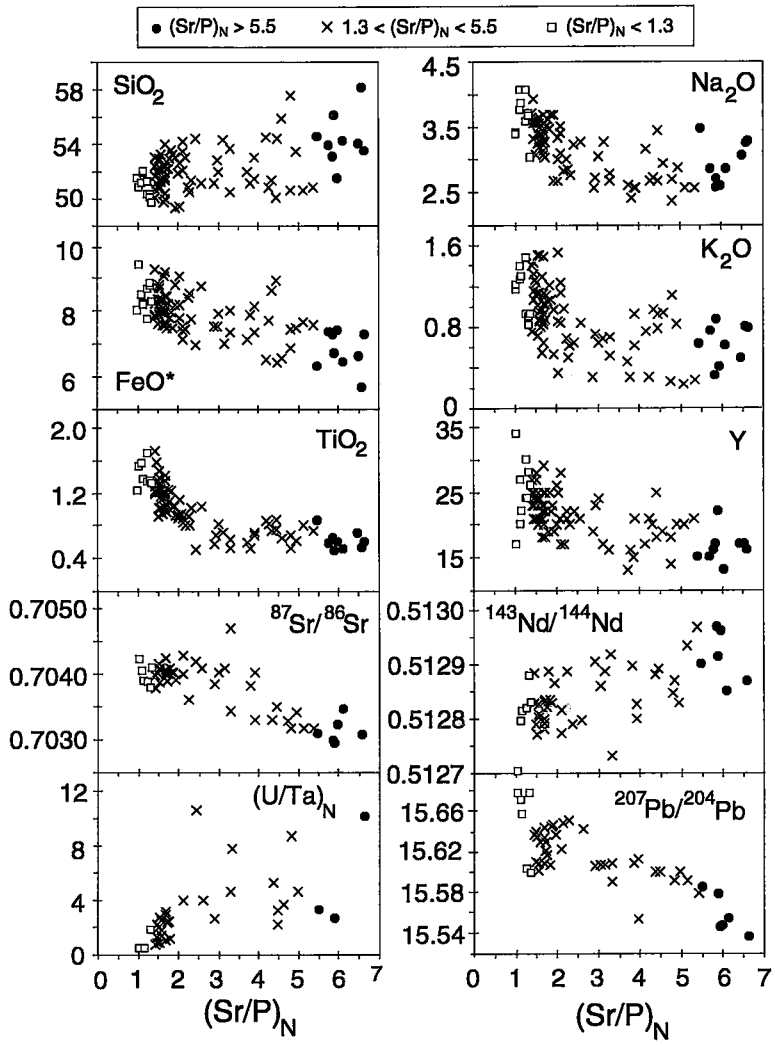

FIG. 6. SiO_2, FeO*, TiO_2, Na_2O, K_2O, Y, $^{87}Sr/^{86}Sr$, $^{143}Nd/^{144}Nd$, $^{207}Pb/^{204}Pb$, and $(U/Ta)_N$ *versus* $(Sr/P)_N$. Symbols as in Figure 2. Inverse correlations between the abundances of incompatible elements and $(Sr/P)_N$ demonstrate that the fluid component is not directly controlling the incompatible-element contents of the lavas, and instead suggest that an increased proportion of fluid promotes greater degrees of partial melting or melting of less fertile peridotites. In contrast, correlations between Sr, Pb, and Nd isotopic ratios and $(Sr/P)_N$ indicate the slab component strongly influences the isotopic composition of the source region of the Lassen lavas.

Sr and Pb isotopic ratios, which decrease with increased SiO_2, and Nd isotopic ratios, which increase with increased SiO_2. Igneous and metamorphic rocks of the upper crust beneath the Lassen region are likely to be isotopically similar to rocks observed in the Sierra Nevada and Klamath mountains, and have Sr isotopic ratios that are too radiogenic (0.7383 to 0.7044), and Nd isotopic ratios that are too unradiogenic [0.51178 to 0.51283; DePaolo (1981), Borg (1995)]. The poor correlation of isotopic ratios, incompatible-element abundances, and incompatible-element ratios with geochemical indices of differentiation suggests that the compositional differences observed in the lavas are not produced by AFC processes. Instead, the relative primitiveness of both lava groups is evidence that the crust has little effect on the composition of the lavas. Since crustal-level processes are unlikely to produce the main geochemical variations in the primitive lavas, we

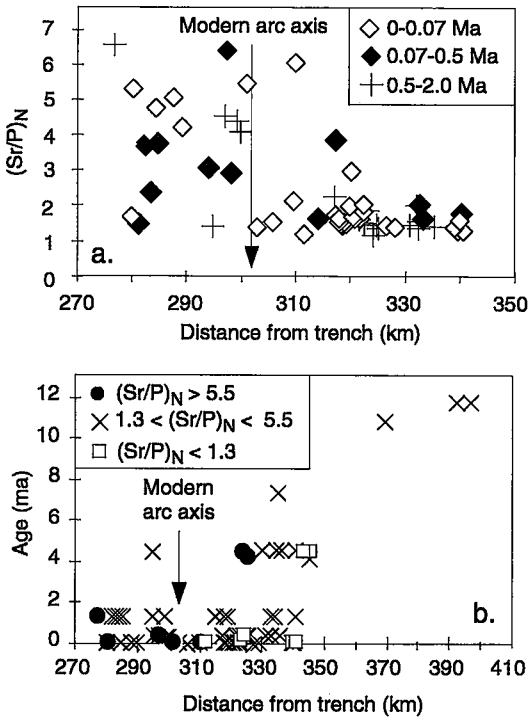

FIG. 7. a. $(Sr/P)_N$ *versus* distance from the trench for lavas with ages ranging from 0 to 0.07 Ma (open diamonds), from 0.07 to 0.5 Ma (solid diamonds), and from 0.5 to 2.0 Ma (crosses). Age estimates from Guffanti *et al.* (1990, and pers. comm.). Lavas with high $(Sr/P)_N$ are observed primarily in the forearc, whereas lavas with low $(Sr/P)_N$ are primarily in the arc axis and backarc regions. b. Age *versus* distance from the trench for all calc-alkaline lavas with $SiO_2 < 55$ wt.%. Symbols as in Figs. 2 and 6. In any given time-slice, the strongly spiked lavas are more abundant in the forearc region, whereas the weakly spiked lavas are more abundant on the arc axis and in the backarc.

conclude that the compositional differences between the strongly and weakly spiked lavas are inherited from their respective sources in the mantle.

High $\delta^{18}O$ values observed in the lavas in the Lassen region, and throughout the Cascade arc, have been attributed to contamination of primitive magmas in the lower crust (Bacon *et al.* 1997). However, generation of high-$\delta^{18}O$ lavas by contamination processes is unlikely, given the lack of correlation between $\delta^{18}O$ and typical indices of differentiation. Furthermore, the high compatible-element content, high Mg#, and simple mineral assemblage of these lavas prohibit significant amounts of crustal interaction, and require potential assimilants to have ultramafic compositions. Tholeiites from the Lassen region also display elevated $\delta^{18}O$, although these lavas show no other evidence of crustal interaction (Bacon *et al.* 1997). We, therefore, conclude that the elevated $\delta^{18}O$ observed in the Lassen lavas are not the result of contamination processes.

Role of subducted sediment

Bullen & Clynne (1990) and Clynne (1993) postulated compositionally diverse sources for the magmas of the southernmost Cascades. They suggested that the sources range from peridotites with incompatible-element contents that are similar to a MORB-source to peridotites that are more similar to an OIB-source. However, all of the Lassen lavas have high Ba/La (15–61), Pb/La (0.14–0.48) and Cs/Rb (0.009–0.05) relative to MORB and OIB [3–10, 0.09–0.12 and 0.013; Sun & McDonough (1989)], suggesting that sediment has been added to the mantle wedge by slab-derived fluids or melts (*e.g.*, Gill 1981). Sediment involvement in many of the lavas is also supported by high $^{207}Pb/^{204}Pb$ values relative to oceanic basalts (Fig. 5). Although the sediment geochemical signature is probably added to the wedge by fluids or melts rising from the slab, the lack of correlation between the sediment signature and virtually any other geochemical features of the lavas, including *LILE/HFSE* and $(Sr/P)_N$, suggests that addition of sediment may not be associated with the current subduction regime. Despite this uncertainty, in this section the role of sediment in magma genesis is evaluated by incompatible element- and isotope-based models. We emphasize that since neither the exact composition of the sediment prior to subduction nor the extent to which the sediment has been compositionally modified by subduction processes is well known, only elements that are least likely to be fractionated (*i.e.*, the most incompatible elements) are modeled.

Estimates of sediment involvement based on Cs/Rb ratios are probably the most useful, because high concentrations of Cs and Rb, and high Cs/Rb, in sediments compared to typical sources in the mantle clearly indicate the presence of small amounts of sediment in the lavas. Average Cs in both terrigenous and pelagic sediments is about 5.7 ppm (Ben Othman *et al.* 1989), compared to N–MORB and OIB values of 0.007 ppm to 0.387 ppm (Sun & McDonough 1989). Furthermore, Cs/Rb will not be strongly affected by partial melting, addition of oceanic crustal partial melts, or addition of slab-derived fluids, as Cs and Rb are not likely to be significantly fractionated by melting or dehydration. As a result, the Cs/Rb value observed in the lavas directly reflects the mixture of sediment and peridotite components in the source region. It will be shown in a later section that other typical indices of sediment involvement such as U/Nb, Pb/La, and Pb isotopic ratios are influenced by the presence of both sediment and slab-derived fluids in the source region, and are therefore not uniquely diagnostic of sediment contributions to the magmas of the southernmost Cascades.

The minimal fractionation of Cs from Rb by partial melting permits Cs/Rb-based binary mixing models of sediment and wedge peridotites to be used to quantify sediment involvement in magma genesis. Peridotites with incompatible-element compositions that are similar to both MORB- and OIB-sources are tested in the model because such sources have been previously postulated to be involved in the petrogenesis of the southernmost Cascade lavas (Bullen & Clynne 1990, Clynne 1990). Although we calculate a compositional range for hypothetical mantle-wedge peridotites from average values for MORB and OIB, we do not mean to imply a genetic relationship between the composition of the wedge peridotites and ocean-basin magmatism. The calculated compositions of the sources simply represent a range of values for the non-subduction-enriched peridotite component in the mantle wedge. The source compositions (hereafter referred to as MORB- and OIB-sources) used in this and the following models (Table 3) are calculated from the average composition of Juan de Fuca N–MORB and Hawaiian tholeiite assuming 5% partial melting of olivine – two-pyroxene peridotites (see caption of Fig. 8 for details of model).

Mixing between average terrigenous and pelagic sediment and MORB-and OIB-sources demonstrates that the total sediment contribution to the magmas of the southernmost Cascades averages about 0.01% for a MORB-source and about 0.3% for an OIB-source (Fig. 8). Minor contributions of sediment are consistent with the absence of a Ce anomaly in the lavas and low B contents of Cascade lavas in general (W. Leeman, pers. comm.). Mixing models demonstrate that a significant Ce anomaly ($Ce/Ce^* < 0.9$) will be produced in the mantle wedge if more than 0.5% sediment (with the composition presented in Table 3) is added to peridotites of MORB-source composition, or if 1% sediment is added to peridotites of OIB-source composition. Therefore, Cs/Rb ratios and Ce/Ce* values of the Lassen lavas are consistent in that they require that the maximum contribution of sediment to the wedge peridotites be less than 1%.

TABLE 3. RESULTS OF PARTIAL MELTING MODELS

	Components of lavas				Weakly spiked lavas		Strongly spiked lavas		Moderately spiked lavas	
	OIB-source (ppm)	MORB-source (ppm)	Pacific Sediment (ppm)†	Fluid (ppm)¥	Lavas $(Sr/P)_N$ <1.3	Sediment-enrichment Model	Lavas $(Sr/P)_N$ >5.5	Slab-fluid enrichment Model I	Lavas $(Sr/P)_N$ 2.2-3.9	Slab-fluid enrichment Model II
Cs	0.009	0.0003	4.90	2	0.44	0.59	0.32	0.33	0.35	0.34
Rb	0.80	0.026	52.0	147	21.0	11.8	14.3	14.9	17.1	12.3
Ba	13.1	0.288	523	1371	463	187	217	146	388	151
Th	0.16	0.0060	11.0	11	2.05	2.60	1.30	1.67	1.67	1.52
U	0.028	0.0025	2.2	4	0.49	0.46	0.58	0.63	0.53	0.51
Nb	1.13	0.12	9.8	46	16.0	17.1	3.4	4.97	7.47	7.83
Ta	0.10	0.0075	0.50	3	1.01	1.04	0.26	0.27	0.42	0.50
K	540	27.7	15175	70559	9463	8231	5230	5545	7330	5740
La	1.48	0.150	33.7	99	20.3	17.8	9.56	10.6	12.8	12.6
Ce	4.45	0.490	21.7	297	45.9	46.9	20.2	27.9	27.9	32.0
Pb	0.17	0.029	23.0	17	3.55	2.79	2.78	2.40	3.00	2.97
Sr	28.7	5.77	254	4681	536	359	649	397	477	407
Nd	2.97	0.654	34.5	147	24.9	26.7	11.4	11.0	15.6	15.8
Sm	1.01	0.293	7.5	35	5.16	7.17	2.40	2.77	3.45	3.78
Zr	26.4	7.2	156	985	164	158	94	98	118	118
Hf	0.60	0.20	2.5	27	3.65	3.67	1.96	2.16	2.54	2.30
Eu	0.26	0.119	1.7	13	1.56	1.59	0.78	0.82	1.07	1.03
Ti	1980	996	5336	85000	8454	12124	3897	4041	5873	5738
Gd	0.86	0.467	7.2	39	4.05	4.12	2.43	2.32	3.13	2.84
Yb	0.56	0.402	3.5	32	2.19	1.88	1.29	1.45	1.79	1.67

Abundances of major and trace elements expressed in ppm. † Gorda Basin sediment data from Davis et al. (1992) and Pacific sediment data from Ben Othman et al. (1989). ¥ Data from Stolper & Newman (1994) and calculated (see text). Sediment-enrichment model reproduced the composition of the weakly-spiked compositional end-member from OIB-source + sediment. Slab-fluid enrichment Model I reproduces the composition of the strongly-spiked compositional end-member from MORB-source + sediment + fluid. Slab-fluid enrichment Model II reproduces the composition of lavas with moderate Sr spikes from mixed MORB-OIB-source + sediment + fluid. See caption of Fig. 9 and Table 4 for model parameters.

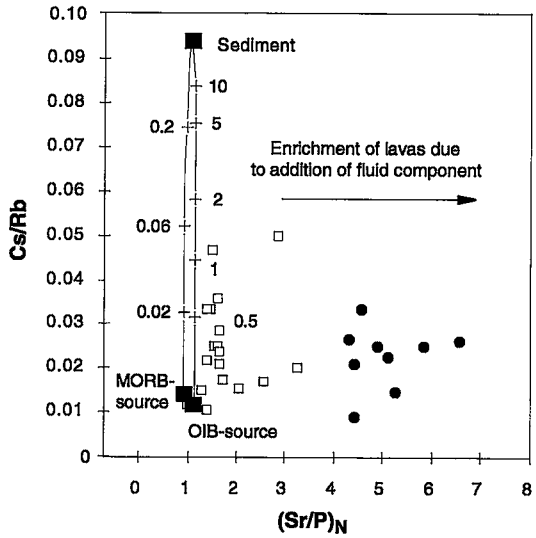

FIG. 8. Model to evaluate the mixing of sediment with MORB-source and OIB-source peridotites. MORB-source composition was calculated assuming that the average N–MORB composition of Sun & McDonough (1989) was generated by 5% melting of spinel harzburgite. The OIB-source composition is calculated using average Hawaiian tholeiites (Clague & Frey 1982, Frey & Clague 1983, Roden *et al.* 1984, Chen & Frey 1985, Tatsumoto *et al.* 1987, Tilling *et al.* 1987), assuming 5% partial melting of garnet lherzolite. Since the average N–MORB and OIB are not primary, their compositions were corrected for differentiation by adding 10% olivine prior to the calculation of source compositions, yielding parental melts with approximately 13 wt.% MgO. Partition coefficients are presented in Table 4. Average oceanic sediment is from Ben Othman *et al.* (1989). Numbers represent the proportion of sediment (%). The ratio Cs/Rb is most representative of sediment involvement, because the abundance of Cs is low in mantle sources, but up to four orders of magnitude higher in typical sediment (Table 3). The model demonstrates that both strongly spiked and weakly spiked lavas contain only small amounts (<1%) of sediment.

A similar range of Cs/Rb ratios and Ce/Ce* values in the strongly and weakly spiked lavas indicates that the sediment contribution is approximately equal in both groups, if they are derived from similar peridotite sources (Fig. 8). On the other hand, if the lavas are derived from different sources (as is suggested below), then the proportion of sediment contributing incompatible elements to the magma must decrease as the peridotite component becomes more depleted. The simplest scenario to explain the observation that lavas derived from different sources have similar Cs/Rb ratios and Ce/Ce* values is that 1) the sediment was added to the wedge peridotite in a previous subduction regime, and 2) the peridotites were subsequently melted to various extents to produce peridotite sources with variable abundances of incompatible elements.

Modeling the petrogenesis of the weakly spiked lavas

Non-modal batch-melting models are constructed using a variety of incompatible elements to determine if the addition of sediment to the peridotites of the mantle wedge alone can produce the compositions of the weakly and strongly spiked lavas. The models attempt to reproduce the incompatible element patterns of the compositional end-members (Fig. 3, Table 2) by partially melting peridotites with compositions reflecting binary mixtures between sediment and either MORB- and OIB-mantle sources. Although we model the sediment contribution to the mantle wedge by bulk addition, sediment is likely to be incorporated in fluids or melts derived from the slab. Nevertheless, the results of the models should not be significantly affected because incompatible elements are unlikely to be strongly fractionated by dehydration or melting processes occurring in the slab. The composition of Gorda Basin sediment (Table 3) is estimated from Davis *et al.* (1992) and Ben Othman *et al.* (1989). Although the addition of the sediment component to the mantle wedge may have occurred prior to the melting events that produced the depleted MORB-source from the more fertile OIB-source (see above), the outcome of the models is unaffected. We emphasize that the compositions of the MORB- and OIB-sources used in the models simply reflect the composition of the non-sediment-enriched component of the mantle wedge.

The modal mineralogy of the mantle source of the weakly spiked lavas is constrained by estimates of pressure and temperature at the site of melt generation above the slab and experimentally determined phase-relations (summarized from Davies & Stevenson 1992). The depth of melting is estimated to be about 100 km, which corresponds to the estimated depth of the slab beneath the arc axis, where most of the weakly spiked lavas are erupted. The temperature is constrained by Peacock's (1993) thermal models for the top of a young (5 Ma) subducting slab, which is similar to the slab subducting beneath the Cascade arc, to be near 1250°C. Such high pressures and temperatures preclude pargasitic amphibole in the source region. As a result, the source is assumed to be a lherzolite with the assemblage Ol + Opx + Cpx + Spl + Grt + Phl. The presence of garnet in the source is suggested by the fact that the slab beneath the arc axis, where most of the weakly spiked lavas are observed, is estimated to be deeper than 85 km (Guffanti *et al.* 1990), and therefore to be within the stability field of garnet. Both garnet and spinel are included in the models because the melt is expected to equilibrate with garnet and then spinel as it rises through the mantle. Garnet is required to lower the *HREE* content of the lavas, whereas spinel has relatively little influence on the calculated composition of

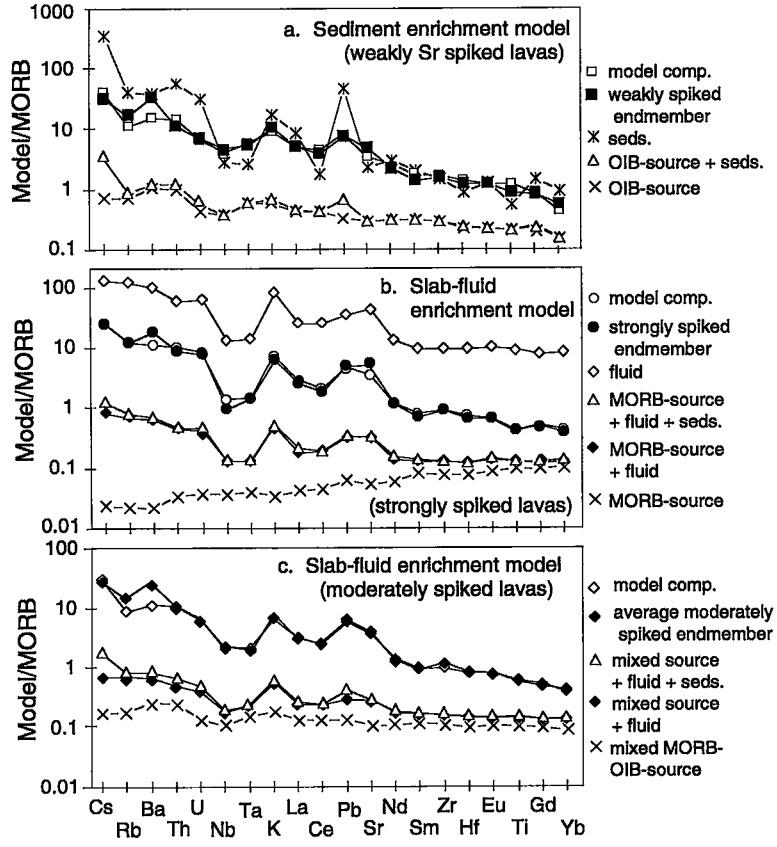

FIG. 9. Sediment- and slab-enrichment batch-melting models. Normalization to N–MORB of Hofmann (1988), with values as follows (in ppm): Cs (0.01408), Rb (1.262), Ba (13.87), Th (0.1871), U (0.0711), Nb (3.507), Ta (0.192), K (883.7), La (3.895), Ce (12.001), P6 (0.489), Sr (113.2), Nd (11.1779), Sm (3.752), Zr (104.24), Hf (2.974), Eu (1.335), Ti (9684), Gd (5.077), and Yb (3.900). Models generate the compositions of Lassen lavas through non-modal melting of peridotites that have been variably enriched through the addition of sediment and fluid from the slab. The composition of sediment is the average measured values of sands, silts, and clays from the Juan de Fuca Basin, taken from Davis *et al.* (1992). In some cases where data are not available for the Juan de Fuca sediments, the average values of Pacific sediment measured by Ben Othman *et al.* (1989) are used. a. Sediment-enrichment model. Crosses are OIB-source (see caption, Fig. 8). Stars are average Pacific sediment (Davis *et al.* 1992, Ben Othman *et al.* 1989). Triangles are sediment-enriched mantle generated by mixing of 99.6% OIB-source and 0.4% average oceanic sediment. Open squares represent composition generated by 8% non-modal partial melting of a lherzolite with Ol:Opx:Cpx:Spl:Grt:Phl = 51:19:19:5:4:2 in the proportions Ol:Opx:Cpx:Spl:Grt:Phl = 11:17:55:1:1:15, with sediment-enriched mantle composition. Solid squares are average composition of the weakly spiked end-member from Table 2 for comparison. This model demonstrates that the weakly spiked lavas can be generated by melting peridotite that has been enriched through the addition of sediment (the strongly spiked lavas cannot be generated in this fashion; not shown on Fig. 9a). It is important to note that although we model the sediment contribution to the Lassen magmas through bulk addition to the mantle wedge, the sediment is likely to be added by fluids or melts derived from the slab. b. Slab – fluid-enrichment model. Crosses are MORB-source (see caption, Fig. 8). Open diamonds represent the composition of the fluid component in Mariana trough magmas, from Stolper & Newman (1994). Solid diamonds are fluid-enriched peridotites calculated by mixing 0.6% fluid component with 99.4% MORB-source mantle. Triangles are peridotites enriched through the addition of both fluid and sediment and are a mixture of 99.31% MORB-source + 0.6% fluid + 0.09% sediment. Open circles are 5% partial melts of fluid-enriched peridotites with Ol:Opx:Cpx:Spl:Grt:Amph = 56:12:6:4:7:15 that has been melted in the proportions Ol:Opx:Cpx:Spl:Grt:Amph = 5:10:45:1:4:35. Closed circles are average composition of the spiked end-member from Table 1. This model demonstrates that the strongly spiked lavas can be produced by melting of amphibole peridotite that has been enriched through the addition of sediment and fluid components. Amphibole in the source has been stabilized by fluid fluxing from the slab. c. Slab – fluid-enrichment model for lavas with moderate Sr spikes. Model parameters intermediate between the models a and b are used. Crosses are peridotite source composed of 75% MORB-source and 25% OIB-source. Solid diamonds are fluid-enriched peridotites calculated by mixing 0.4% fluid component with 99.6% peridotite. Triangles are peridotites enriched through the addition of both fluid and sediment and are a mixture of 99.3% MORB–OIB-mixed source + 0.4% fluid + 0.3% sediment. Open diamonds are 6% partial melts of (fluid + sediment)-enriched peridotites with Ol:Opx:Cpx:Spl:Grt:Amph:Phl = 52:13:20:4:4:6:1 that has been melted in the proportions Ol:Opx:Cpx:Spl:Grt:Amph:Phl = 5:10:46:1:3:25:10. Closed diamonds are average composition of lavas with $2.2 < (Sr/P)_N < 3.9$. The fact that this model is able to reproduce the lavas with compositions intermediate between the strongly spiked and weakly spiked end-members using intermediate model parameters suggests that the compositional continuum observed in the lavas suite reflects the variable involvement of fluids in magma genesis.

TABLE 4. PARTITION COEFFICIENTS USED IN MELTING MODELS

	Ol	Opx	Cpx	Grt	Spl	Amph (pargasite)	Phl
Cs	0.000434	0.001[a]	0.0024	0.001[a]	0	0.14[h]	3.06[h]
Rb	0.000183,4	0.001[a]	0.00192,4	0.0012	0	0.1413	3.0611
Ba	0.00011[4]	0.0005[a]	0.000688	0.0012	0	0.1213	1.0911
Th	0.000255	0.00255	0.015	0.000013	0.00017[10]	0.01713	0.3112
U	0.00013	0.0015	0.025	0.000013	0.00011[10]	0.089	0.31[i]
Nb	0.013	0.025[a]	0.0057	0.047	0.01[d]	0.213	0
Ta	0.01[g]	0.025[g]	0.0137	0.157	0.01[d]	0.2113	0
K	0.000184	0.0011[a]	0.00222,4	0.0012	0	0.3311	2.712
La	0.00043	0.0256	0.052	0.013	0.013	0.173	0.036[e]
Ce	0.0081	0.0041	0.151	0.0281	0.013	0.2213	0.03411
Pb	0.00013	0.001333	0.013	0.00053	0	0.1213	0
Sr	0.00023	0.0073	0.0782	0.012	0	0.123	0.08111
Nd	0.0091	0.0081	0.171	0.0681	0.013	0.6213	0.03211
Sm	0.00951	0.0161	0.261	0.291	0.013	0.6613	0.03111
Zr	0.01[b]	0.187	0.36	0.57	0.07	0.2313	2.112
Hf	0.013	0.13	0.36	0.36	0.07	0.4513	2.1j
Eu	0.011	0.0211	0.281	0.491	0.013	0.883	0.0311
Ti	0.0063	0.0243	0.32[d]	0.42	0.0483	2.0213	0
Gd	0.01071	0.0261	0.321	0.971	0.013	0.863	0.0311
Yb	0.0161	0.11	0.291	51	0.013	0.593	0.04211

Reference
1. DePaolo (1988)
2. Kay (1978)
3. McKenzie & O'Nions (1991)
4. Hart & Brooks (1974)
5. Meijer et al. (1990)
6. Lowest values of range from Wilson (1989)
7. Green et al. (1989)
8. Hart & Dunn (1993)
9. Le Marchand et al. (1987)
10. Beattie (1993)
11. Arth (1976)
12. Biotite from Henderson (1982)
13. Brenan et al. (1995)

Calculation
a. Ratioed to cpx.
b. Same as Hf.
c. Same as olivine KD.
d. Same as Gd.
e. Ratioed to Cs/Rb, Hf/Zr, Nb/Ta, or HREE/Sm in evolved crustal rocks.
f. Ratioed to average of Ti/Eu and Ti/Gd in N-MORB.
g. same as Nb.
h. same as Rb.
i. same as Th
j. same as Zr

the melt. We emphasize that although the models assume both garnet and spinel in the residuum, each phase is stable at a different depth, and therefore time in the history of the melt. Phlogopite is assumed to be present in the peridotite because it is the only common hydrous phase that is stable in the wedge beneath the arc axis once the stability field of amphibole is exceeded, at about 85 km in the forearc. In addition, phlogopite is a likely by-product of amphibole breakdown (Green 1973). The high compatibility of K, Rb, and Ba in phlogopite (and most other K-rich phases), combined with the absence of K, Rb, and Ba depletions in the lavas (Fig. 3), suggest that, if present, a significant proportion of it melts.

Non-modal batch-melting models of lherzolite enriched by the bulk addition of sediment replicate the overall incompatible-element composition of the weakly spiked end-member in Table 2. The best-fit model (see caption to Fig. 9a, Table 3) requires 8% non-modal partial melting, in the proportions Ol:Opx:Cpx:Spl:Grt:Phl = 11:17:55:1:1:15, of a lherzolite with Ol:Opx:Cpx:Spl:Grt:Phl = 51:19:19:5:4:2 and an OIB-source composition prior to enrichment through the addition of 0.4% sediment (partition coefficients in Table 4). Thus, the composition of the modeled peridotite is a mixture of 99.6% OIB source + 0.4% sediment.

Partial melting models that use a MORB-source (instead of a OIB-source) that has been enriched through the addition of sediment do not reproduce the composition of the weakly spiked end-member. If 0.4% sediment is added to a MORB-source, then extremely small amounts of melting (<0.5%) are required to generate the overall abundances of incompatible elements of the weakly spiked end-member. The best-fit model composition has abundances of Rb, Ba, and K, and a Cs/Rb value, that are 200 to 400% lower than the weakly spiked end-member composition, and abundances of Th, U, and Pb that are 100% too high. Conversely, the addition of 1.5% sediment is required for 3% partial melting of a MORB-source mantle. This much sediment generates modeled melts with Pb abundances, Ce anomalies and Cs/Rb ratios that are significantly greater than values observed in the weakly spiked end-member, whereas modeled Sr abundances are significantly lower. Thus, the models are unable to reproduce the compositions of the weakly spiked end-member from a MORB-source composition, despite the use of either small degrees of melting or addition of large amounts of sediment. However, the fact that the weakly spiked lavas cannot be generated from a MORB-source does not preclude its presence in the mantle wedge.

The isotopic compositions of the weakly spiked lavas are consistent with derivation from an OIB-source peridotite as well. By assuming a reasonable isotopic composition of the sediment component, the isotopic composition of the peridotites required to generate the weakly spiked end-member can be calculated, since the proportions of Sr, Nd and Pb from peridotite and sediment are constrained by the models. The average measured Sr and Nd isotopic composition of Pacific sediment is given by: $^{87}Sr/^{86}Sr = 0.70976$, $^{143}Nd/^{144}Nd = 0.51234$ (Ben Othman *et al.* 1989). The average Pb isotopic composition of Gorda Basin sediment is given by: $^{208}Pb/^{204}Pb = 38.85$, $^{207}Pb/^{204}Pb = 15.63$, $^{206}Pb/^{204}Pb = 18.93$ (Church 1976). The isotopic composition of pre-sediment-enriched wedge peridotites calculated using these values are similar to some OIB worldwide [$^{87}Sr/^{86}Sr = 0.7038$, $^{143}Nd/^{144}Nd = 0.51284$, $^{208}Pb/^{204}Pb = 38.58$, $^{207}Pb/^{204}Pb = 15.66$ and $^{206}Pb/^{204}Pb = 18.98$; Zindler & Hart (1986), Hart (1988)]. Nevertheless, the calculated $^{207}Pb/^{204}Pb$ value of the wedge peridotites is higher than pristine (NHRL-like) oceanic mantle, indicating that the $^{207}Pb/^{204}Pb$ value assumed for the sediment is too low. Sediments with higher $^{207}Pb/^{204}Pb$ values have not been observed in the region (Fig. 5), suggesting that a previous (non-Cascadia) enrichment of the wedge peridotites by another sedimentary component with higher $^{207}Pb/^{204}Pb$ value may have occurred. This is consistent with the observation that the geochemical signature of the sediment does not correlate with the modern subduction signature [*e.g.*, *LILE/HFSE* and $(Sr/P)_N$], nor vary across the southernmost segment of the arc.

Unlike the weakly spiked end-member, the composition of the strongly spiked end-member cannot be reproduced by the sediment-enrichment model, even if the mineralogy, degree of partial melting, composition of the peridotite, or amount of sediment is varied dramatically. This stems from the fact that the addition of sediment to the wedge peridotites raises the levels of *LILE* and *LREE* of subsequent melts, but cannot generate the Sr spike nor the Ta–Nb trough observed in the strongly spiked lavas. Whereas the weakly spiked end-

member can be derived by partial melting of sediment-enriched lherzolite with an OIB-source composition, the generation of the strongly spiked end-member requires an additional component.

The slab source of the Sr spike

The fact that $(Sr/P)_N$ is inversely correlated with $^{87}Sr/^{86}Sr$ (Fig. 6) indicates that the excess Sr in the strongly spiked lavas is derived from an unradiogenic source. Radiogenic sources of Sr, including seawater, the upper continental crust, and subducted sediments, can be eliminated on this basis. The fact that the strongly spiked end-member has a $^{87}Sr/^{86}Sr$ value of 0.7031 requires that the $^{87}Sr/^{86}Sr$ of the excess Sr must be at least 0.7031. The $^{87}Sr/^{86}Sr$ value required to generate the average isotopic composition of the Sr spike can be estimated by assuming that 1) the Sr spikes are generated completely by the addition of the high-Sr component, and 2) the strongly spiked lavas are derived from peridotites with $^{87}Sr/^{86}Sr$ similar to the weakly spiked lavas. (The validity of these assumptions is supported by partial melting models developed in the following section that demonstrate that over 80% of the Sr observed in the strongly spiked end-member is derived from dehydration of the slab, and that the isotopic composition of strongly spiked lavas is therefore dominated by the slab component). If the source of the strongly spiked lavas had a smooth incompatible-element pattern prior to addition of the excess Sr, then the $^{87}Sr/^{86}Sr$ value of the added Sr must be approximately 0.7027.

Although it was previously suggested that the peridotite from which the weakly spiked lavas are derived had an OIB-source geochemical and isotopic composition, it is possible that the mantle wedge contains some additional domains of peridotite (that are not involved in the magma genesis of the weakly spiked lavas) with MORB-source compositions and isotopic ratios (Bullen & Clynne 1990, Clynne 1993). Possible arc sources of Sr with $^{87}Sr/^{86}Sr$ near 0.7027 therefore include peridotites with MORB-source compositions and isotopic ratios in the mantle wedge and the subducted slab. Although a MORB-source may have $^{87}Sr/^{86}Sr$ that is low enough to serve as the source of the excess Sr, it is unlikely that the unradiogenic Sr is derived from the mantle wedge, since melting of peridotites cannot significantly separate Sr from P or *LREE* (*e.g.*, Thompson *et al.* 1984, Sun & McDonough 1989, McKenzie & O'Nions 1991). Only the subducted oceanic crust is both unradiogenic enough to provide the strongly spiked lavas with excess Sr and potentially be able to fractionate Sr from other incompatible elements *via* dehydration or possibly melting reactions. Furthermore, high concentrations of Sr in the Gorda Basin and Juan de Fuca basalts (average Sr = 134 ppm; Hofmann & White 1983, Hegner & Tatsumoto 1987), combined with continued subduction for tens of millions of years, make the subducting slab the largest potential reservoir of unradiogenic Sr in the arc system.

Modeling the petrogenesis of strongly spiked lavas

The first step of any petrogenetic model for the strongly spiked lavas is to provide a mechanism to transport unradiogenic Sr from the subducted oceanic crust and preferentially enrich it over incompatible elements such as Nd and P in the source. Both small-volume partial melts of eclogitic slab, and fluids released by dehydration of the amphibolitic slab, have been proposed as the medium by which the slab fluxes the mantle wedge with incompatible elements, preferentially enriching the wedge in Sr (*e.g.*, Kay 1978, Stern *et al.* 1984, Defant & Drummond 1990a, b, Kay *et al.* 1991, 1993, Stolper & Newman 1994, Yogodzinski *et al.* 1994). The observation that the strongly spiked lavas are concentrated in the forearc firmly constrains the enrichment mechanism. Although the young age of the Juan de Fuca plate and the slow rate of subduction make the Cascade subduction zone extremely hot, dry melting of eclogitic rocks is unlikely to be the source of the Sr spike. Temperatures near 1375°C are required at the slab–wedge interface to exceed the dry basalt (eclogite) solidus at 80–90 km depth in the forearc (*e.g.*, Lambert & Wyllie 1972). Similar or higher temperatures are therefore expected beneath the arc axis, resulting in dehydration of the slab–wedge interface. Such high temperatures beneath the arc axis, however, are not consistent with the abundance of relatively volatile-rich magmas in this region or thermal models for the Cascade subduction zone (Connard *et al.* 1984, Lewis *et al.* 1989, Hyndman & Wang 1993, Peacock 1993). Furthermore, melts of eclogite (Cpx + Grt) are unlikely to have both enrichments in Pb and depletions in Ta and Nb, and therefore cannot produce the geochemical signatures of the strongly spiked lavas.

Fluxing the mantle wedge with volatiles derived from dehydration reactions in the subducting slab is the most common mechanism invoked to explain both the initiation of magmatism in volcanic arcs and the relatively constant depth of the slab beneath volcanic fronts worldwide (*e.g.*, Gill 1981). Dehydration experiments and thermal models demonstrate that the transition from amphibolite to eclogite facies in the slab normally occurs beneath the forearc (*e.g.*, Gill 1981, Tatsumi 1989). Experimentally determined phase-relations (summarized from Davies & Stevenson 1992) and thermal models for the top of a young (5 Ma) subducting slab, similar to the slab subducting beneath the southernmost Cascade arc (Peacock 1993), indicate, however, that amphibole in the top of the slab will dehydrate at around 65 km and 1000°C or just west of the Lassen forearc. Fluid released from dehydration of amphibole in the slab at relatively shallow depths may be downdragged deeper into the sub-arc mantle by corner flow of the wedge peridotites (Tatsumi 1986,

1989). As a result, fluid is expected to be present in the Lassen forearc, and may account for the geochemical signatures of the strongly spiked lavas.

Generation of Sr spikes through the enrichment of the mantle wedge by slab-derived fluid can be tested using batch-melting models. The construction of these models is similar to the non-modal melting models presented in the previous section, except that the wedge is assumed to be a mixture of peridotite with a MORB-source composition, sediment, and slab-derived fluid that is subsequently melted to produce the magmas (see caption of Fig. 9b for details of the model). The source peridotites for the strongly spiked lavas probably have mineralogical and geochemical affinities with a MORB-source, which is supported by the presence of high-Mg# silicates and spinels observed in these lavas (Clynne & Borg 1997). However, the likely presence of OIB-source peridotites in the mantle wedge (see above) requires that the potential role of this source be investigated as well.

The presence of a hydrous phase in the source region is implied by the fluxing of the mantle wedge in the forearc with fluids. Experimentally determined phase-relations demonstrate that pargasitic hornblende is stable to depths around 85 km and 1175°C in the peridotites of the mantle wedge (Lambert & Wyllie 1972, Millhollen *et al.* 1974, Rapp *et al.* 1991, Rushmer 1991, Davies & Stevenson 1992, Dunn *et al.* 1993, Pawley & Holloway 1993). The fact that lherzolite xenoliths from Ichinomegata crater in northeastern Japan commonly contain pargasitic hornblende confirms both the hydrated nature of at least some sub-arc mantle and the presence of amphibole (Takahashi 1980, 1986, Aoki 1971). The steep geotherm beneath the Lassen region requires that the stability of amphibole in the mantle wedge be controlled by the amphibole-buffered peridotite solidus and not by pressure-sensitive dehydration (Davies & Stevenson 1992). In other words, the P–T path for the down-dragged peridotites just above the subducting slab intersects the vertical portion of the amphibole-out curve (see Fig. 6 in Davies & Stevenson 1992). As a result, amphibole is expected to be present and participate in melting reactions beneath the Lassen forearc. The higher temperatures expected at the slab–wedge interface beneath the arc axis are likely to confine amphibole to the forearc. As in the previous models of the weakly spiked end-member, both garnet and spinel are used to simulate progressive equilibrium of the melt with first garnet, and then spinel, peridotite as it rises upward through the mantle wedge. The proportion of phases modeled in the source is Ol:Opx:Cpx:Spl:Grt:Amph = 56:12:6:4:7:15, and is similar to the proportions observed in hydrated lherzolite xenoliths from Japan (*e.g.*, Lhz 13 has Ol:Opx:Cpx:Spl:Amph = 62:21:6:2:9) by Takahashi (1980).

Although the fluid derived from the slab is probably a mixture of both oceanic crust and sediment components, the lack of correlation between the geochemical signatures of the fluid and sediment [*e.g.*, Cs/Rb and $(Sr/P)_N$] in the lavas suggests a previous enrichment of the mantle wedge by the sediment component (see above). As a result, addition of sediment and fluid to the wedge are modeled as independent processes. The contribution of sediment is again modeled by bulk addition to the wedge peridotites because the effects of melting and dehydration in the slab are unconstrained, but probably minimal for the incompatible elements used in the models.

The main difficulty with these models is determining realistic incompatible-element abundances for the slab-derived fluid. Stolper & Newman (1994) have estimated the composition of the slab-derived fluid component in magmas associated with the Mariana trough using mass-balance techniques, and assumed that the fluid-rich lavas were derived from a calculated N–MORB source. The composition of the fluid used in the model presented here is from Stolper & Newman (1994). Note that Cs, Nb, Ce, Eu, Hf, Ti, and *HREE* of the fluids were not estimated by Stolper & Newman (1994), and are therefore calculated by assuming that the ratios Cs/Rb, Nb/Ta, Ce/La, Eu/Sm, Hf/Zr, Ti/Sm, and *HREE*/Sm have the same values in the fluid as in N–MORB. Normalizing these elements to N–MORB (instead of sediment) does not significantly change the results of the models, and is probably more reasonable because in the models a sediment component is added to the wedge peridotites separately. Although this fluid may not be directly applicable to the Lassen lavas, it serves as a first approximation to determine if generation of the Sr spikes by the addition of slab fluids is reasonable. We note that the fluid is characterized by high Sr and low Ta and Nb (Fig. 9b, Table 3), and therefore has the appropriate overall geochemical signature.

Whereas the amount of fluid is constrained by the Sr/*LREE* value of the strongly spiked end-member, and the amount of sediment is constrained by the Cs/Rb value, the composition of the peridotite source is not known. As a result, models based upon peridotites with both MORB-source and OIB-source compositions are constructed. Models based upon MORB-source compositions can reproduce the composition of the strongly spiked lavas. The best-fit model (Fig. 9b, Table 3) requires 5% partial melting of peridotites with a composition represented by a mixture of 99.31% MORB-source + 0.6% fluid + 0.09% sediment. The peridotite is melted in the proportions Ol:Opx:Cpx:Spl:Grt:Amph = 5:10:45:1:4:35 (and is modeled to contain Ol:Opx:Cpx:Spl:Grt:Amph = 56:12:6:4:7:15; see caption of Fig. 9b for details). The incompatible-element pattern produced by this model closely resembles the pattern observed in the strongly spiked lavas, and has a large Sr enrichment and Nb and Ta depletions. The modeled concentration for most elements is within 15% of the values of the strongly spiked end-member (Fig. 3, Table 3). Nevertheless, the Sr spikes produced by the models are about 60% lower than the Sr spike of the end-member composition. Adding more fluid to the wedge will not pro-

duce all the Sr enrichment observed in the strongly spiked end-member because the fluid has lower Sr/*LREE* than the end-member. It is more likely that the fluid component that is present in the Lassen source-region has more Sr than the fluid calculated in Mariana trough magmas. A fluid with about 75% more Sr is required to reproduce the Sr abundance of the strongly spiked end-member.

Models based upon an OIB-source composition and reasonable modes in the source cannot reproduce the composition of the strongly spiked end-member. Incompatible-element patterns produced by this model lack the Sr enrichment and Ta and Nb depletions that characterize the strongly spiked lavas, even if the amount of fluid, sediment, and degree of melting are drastically varied. The only way to generate incompatible element patterns that resemble the pattern of the strongly spiked lavas is to use a source that contains very large amounts of amphibole (>55%). It is therefore unlikely that the strongly spiked lavas are produced by melting an OIB-source that has been enriched through the addition of slab components.

Generation of the compositional continuum between end-member lavas

The good correlation between the Sr spike and Ta and Nb troughs on normalized spidergrams (Fig. 6) suggests that the presence of fluid is responsible for the depletion of Ta and Nb relative to *LILE* and *LREE* observed in the lavas. The partial melting models generate the Ta and Nb troughs observed in the strongly spiked lavas through 1) the addition of the high-*LILE*, high-*REE*, low Ta and Nb fluid component, and 2) the slightly greater compatibility of Ta and Nb in amphibole relative to the other phases postulated to be present in the mantle wedge (Brenan *et al.* 1995). Note that the amphibole (pargasite)–melt partition coefficients for Ta and Nb that are used in the model are fairly conservative ($K_D^{Amph/melt}$ = 0.2) compared to some other published values (*e.g.*, $K_D^{Amph/melt}$ = 0.8; Witt-Eickschen & Harte 1994). Although the two mechanisms for the generation of the Ta and Nb depletions cannot be distinguished, they may both be required to produce the observed troughs. If the fluid has $(K/Nb)_N$ = 1.0, then the $K_D^{Amph/melt}$ for Nb would have to be very high (near 4), suggesting that the fluid must be depleted in Nb relative to *LILE* and *REE*. In contrast, if amphibole was not present in the source region, then the fluid is required to have Nb concentrations and Nb/K ratios that are 20 times lower than has been postulated by Stolper & Newman (1994).

The compositions of the strongly spiked lavas are consistent with a large contribution of slab-derived fluid and a relatively large proportion of amphibole in the source, whereas the compositions of the weakly spiked lavas are successfully modeled by melting peridotite in the absence of both fluid from the slab and amphibole in the source. Thus, the compositional continuum between the strongly and weakly spiked lavas is likely to reflect the abundance of fluid added to the mantle wedge from the slab. This is supported by the fact that the compositions of moderately spiked lavas with $2.2 < (Sr/P)_N < 3.9$ [average $(Sr/P)_N$ = 2.7] can be modeled with an intermediate amount of fluid and proportion of amphibole in the source (Fig. 9c). We therefore suggest that the variable contribution of fluid to the mantle wedge produces the varied arc geochemical signature observed in the Lassen lavas by adding incompatible elements to the source region of the magma (producing most notably the Sr spike and much of the Ta and Nb troughs), and possibly through stabilization of amphibole (which may help to produce the remainder of the Ta and Nb troughs).

DISCUSSION

In this section, the melting models developed in the previous section are used to evaluate the sources of incompatible elements in the lavas. Since the models do not strongly constrain the trace-element composition of the peridotite component in the wedge, abundances of major elements are used to assess whether the range of incompatible-element abundances observed in the lavas is produced by melting of peridotites with varied compositions, or by varying degrees of melting.

Sources of incompatible elements

The concentrations of incompatible elements observed in a lava reflect 1) the proportion of slab (sediment and fluid) and peridotite components involved in magma genesis, 2) the abundance of incompatible elements in these components, 3) the mineralogy of the source, 4) the degree of partial melting, and 5) differentiation. In the case of the southernmost Cascades, the slab component has been divided into a fluid component, which has been added to the wedge in the current subduction regime, and a sediment component, which appears to reflect a previous subduction event. If we assume the compositions of fluid, sediment, and peridotite components, our models dictate the fraction of each individual incompatible element derived from these three components (Table 5). This analysis is independent of differentiation, because differentiation is unlikely to fractionate incompatible elements from one another. From Table 5, it is apparent that the primary sources of incompatible elements are element-specific. The concentrations of some elements in the lavas, such as Pb and Cs, are strongly dependent on the proportion of sediment added to the source. This results from high concentrations of these elements in sediments relative to the fluid and peridotite components. Other elements, such as Sr, Rb, Ba, U, and K, are preferentially enriched in the fluid component over the sediment and peridotite components, and are therefore

TABLE 5. SOURCES OF INCOMPATIBLE ELEMENTS

	Sediment-Enrichment Model		Slab-Fluid Enrichment Model I		
	Peridotite	Sediment	Fluid	Peridotite	Sediment
Cs	27	73	72	2	26
Rb	75	25	92	3	5
Ba	83	17	92	3	5
Th	75	25	82	7	11
U	72	28	86	8	6
Nb	96	4	69	29	2
Ta	98	2	68	30	2
K	88	12	91	6	3
La	90	10	78	18	4
Ce	98	2	79	20	1
Pb	41	59	69	18	13
Sr	96	7	83	16	1
Nd	94	6	54	44	2
Sm	96	4	43	56	1
Zr	97	3	47	52	1
Hf	98	2	47	52	1
Eu	97	3	42	57	1
Ti	99	1	36	63	1
Gd	96	4	35	64	1
Yb	97	3	34	65	1

Numbers represent percent derived from fluid, peridotite, and sediment sources as required by melting models.

primarily derived from the fluid. Finally, elements such as the heavy-*REE* and *HFSE* are in relatively low concentrations in the sediment and fluid components, and are mostly derived from the peridotites.

Like the incompatible elements in the southernmost Cascade lavas, the isotopic composition is determined by the mixture of fluid, peridotite, and sediment components. The isotopic composition of the fluid component can be estimated using the proportions of Sr, Nd, and Pb derived from fluid, MORB-source, and sediment components as determined by the melting models for the strongly spiked end-member. This application requires that the isotopic composition of the sediment and peridotite be known, however. The fact that $^{87}Sr/^{86}Sr$ negatively correlates with the fluid geochemical signature [*e.g.*, $(Sr/P)_N$] indicates that the Sr isotopic composition of the fluid is lower than the Sr isotopic composition of the sediment-enriched MORB-source. Thus, the peridotite source of the strongly spiked lavas is similar to MORB-source in terms of its incompatible-element contents only, but not in terms of its isotopic composition. If we assume that 1) the isotopic compositions calculated for the OIB-source peridotites of the weakly spiked lavas (see above) represent the average isotopic composition of all the mantle-wedge peridotites, and 2) the isotopic composition of the sediments is similar to that of the Gorda Basin sediment, then the isotopic composition of the fluid can be estimated by mass balance. Its isotopic composition is estimated to be: $^{87}Sr/^{86}Sr$ = 0.7028, $^{143}Nd/^{144}Nd$ = 0.51307, $^{208}Pb/^{204}Pb$ = 38.13, $^{207}Pb/^{204}Pb$ = 15.52, and $^{206}Pb/^{204}Pb$ = 18.69. The calculated Sr, Nd and Pb isotopic values of the fluid fall within the Juan de Fuca MORB field, and are therefore consistent with derivation of the fluid from the subducted slab.

From Table 5, it is apparent that the isotopic composition of the lavas is strongly influenced by the presence of the fluid component. The geochemical models require up to 83% of the Sr, 54% of the Nd, and 69% of the Pb to be derived from the fluid released from the slab (Table 5). The isotopic composition of arc magmas derived from fluid-rich sources may therefore be dominated by the fluid component, and only vaguely reflect either the presence of sediment or the composition of the wedge peridotites. Thus, increasing the fluid contribution simultaneously raises the Sr spike and gives the resulting magma a more MORB-like isotopic signature. Strongly spiked lavas have MORB-like Sr and Pb isotopic signatures, but less radiogenic Nd, as a result of the fact that the slab component is more enriched in Sr and Pb than Nd. The most strongly spiked lavas, therefore, fall to the left of the Sr–Nd mantle array (Fig. 4).

Compositional variability versus partial melting of the mantle wedge

Although slab-derived fluids have high concentrations of incompatible elements, the strongly spiked lavas are characterized by lower abundances of most incompatible elements than the weakly spiked lavas. The presence of the fluid component, therefore, does not significantly raise the incompatible-element content of the strongly spiked lavas. Instead, the observed inverse correlation between $(Sr/P)_N$ and incompatible-element abundances (Fig. 6) suggests that the presence of the slab component results in either greater amounts of partial melting or melting of more depleted mantle (*e.g.*, Clynne 1993, Luhr 1993). Although our models account for the variable incompatible-element contents of the strongly and weakly spiked lavas by similar degrees of melting of MORB-and OIB-source peridotites, and are unable to produce both the strongly and weakly spiked lavas from a single peridotite source, they do not preclude the possibility that the lavas are derived from variable degrees of melting of a single peridotite source that has a composition not considered in the models. In this section, we use major-element compositions of the lavas to evaluate the potential for variable degrees of melting. We confine this discussion to the major elements, because they are less likely than trace elements to be controlled by the addition of small amounts of slab components.

Klein & Langmuir (1987) and Plank & Langmuir (1988) have compared normalized major-element compositions of MORB and arc lavas to the compositions of experimentally produced melts in order to constrain chemical and physical conditions in the mantle during melting. The compositional effects of varying degrees of partial melting and initial peridotite composition on the major-element compositions of melts were determined from experiments on spinel lherzolites by Jaques

TABLE 6. SUMMARY OF EXPERIMENTAL MELTING RESULTS

Element	Decreasing the degree of partial melting	Increasing the fertility of peridotite	Difference between spiked- and unspiked-lavas
Fe	no change	increase	spiked < unspiked
Ti	increase	increase	spiked < unspiked
Na	increase	increase	spiked < unspiked
K	increase	increase	spiked < unspiked
Al	increase	increase	spiked ≤ unspiked
Si	decrease	decrease	spiked > unspiked
Mg	decrease	decrease	spiked > unspiked
Ca	decrease	little or no change	spiked > unspiked

Summarized from Klein & Langmuir (1987) and experimental data of Dunn & Stolper (1993), Fujii & Scarfe (1985) and Jaques & Green (1980).

& Green (1980) and Fujii & Scarfe (1985), and were summarized in Klein & Langmuir (1987). These data are presented in Table 6, along with additional experimental data from Dunn *et al.* (1993). On the basis of this summary, lower abundances of Na, K, and Ti, and higher abundances of Si and Mg in the strongly spiked lavas, relative to the weakly spiked lavas (Figs. 2, 6), are in accord with both higher degrees of melting and lower abundances of incompatible elements in the source of the strongly spiked lava relative to the source of the weakly spiked lava. These elements, therefore, cannot be used to distinguish between the effects of melting and source composition on magma chemistry. In contrast, similar Ca contents in the strongly and weakly spiked lavas (Fig. 2, Table 2) suggest that they are derived by similar degrees of partial melting (Table 6). Lack of correlation between CaO and $(Sr/P)_N$ further suggests that the presence of fluid does not significantly affect the degree of melting. This is supported by higher FeO* of the weakly spiked lavas (Figs. 2, 6), which cannot result from varying degrees of partial melting since extents of partial melting will not significantly alter the abundance of FeO* in the lavas (Table 6). Instead, FeO* is expected to reflect the FeO* abundance of the peridotites (Klein & Langmuir 1987). The higher FeO* contents of the weakly spiked lavas relative to the strongly spiked lavas therefore suggest that the weakly spiked lavas are derived from a more fertile source (*i.e.*, OIB-source), with a higher FeO*, and that the strongly spiked lavas are derived from a more depleted source (*i.e.*, MORB-source), with a lower FeO*.

Correlations between $(Sr/P)_N$ and FeO* of primitive lavas (Fig. 6) suggest that the composition of the source varies with the amount of fluid component in the source region. Fluid-rich sources are generally less fertile (MORB-source) peridotites with low abundances of FeO* and higher-Mg# phases, whereas fluid-poor sources tend to be more fertile (OIB-source) peridotites with higher abundances of FeO* and lower-Mg# phases. This generalization is consistent with mineral-composition data, which indicate the presence of more refractory Mg-rich phases in the strongly spiked lavas (Clynne & Borg 1997). The correlation between the amount of fluid in the source and its inferred relative fertility may reflect the ability of larger proportions of fluid to promote melting of more refractory peridotites with higher-Mg# phases.

Petrogenetic Model for Magmatism in the Southernmost Cascades

The compositional variability of the Lassen lavas reflects a complex relationship between the proportion of the slab component and related variations in the composition of the peridotite component. The strongly spiked lavas of the forearc region are derived from peridotites with a MORB-source composition that have been fluxed by large amounts of slab-derived fluid. The weakly spiked lavas that erupted along the arc axis and in the backarc regions are derived by similar degrees of partial melting of peridotites with a more fertile OIB-source composition, and have a much smaller fluid-contributed component. Any petrogenetic model of magma genesis in the Lassen region must account for these conclusions by correlating variations in the role of the fluid component with mineralogical and compositional changes in the wedge peridotites, as required by the geochemical models. In addition, the petrogenetic model must provide a mechanism to transport fluid into the wedge beneath the forearc region, as well as to account for the steady decrease of the fluid-contributed geochemical signature toward the backarc.

The proposed model is presented in Figures 10a and 10b. The temperature at the slab–wedge interface is constrained by Peacock's (1993) thermal model for the top of a young (5 Ma) oceanic lithosphere that is slowly being subducted. The subsolidus breakdown of amphibole in the slab between 40 and 70 km transfers Sr, Pb, and other incompatible elements to the mantle wedge *via* a fluid phase, stabilizing pargasitic amphibole. Experimentally determined solidi of amphibole-bearing peridotite intersect the thermal model for the top of the subducting slab around 1150°C and a depth of about 80 km (Davies & Stevenson 1992). This is consistent with the depth of the slab beneath the forearc region, estimated to be 85 km by Guffanti *et al.* (1990; Fig. 1c). We therefore propose that melting of amphibole-bearing peridotites initiates magmatism in the forearc region.

Melts of amphibole-bearing peridotites in the forearc are characterized by Sr enrichments and Ta and Nb depletions (reflecting incompatible-element enrichment by fluids and, possibly, greater compatibility of Ta and Nb in amphibole). Amphibole in the residuum is reasonable since the amphibole-out reaction is controlled by temperature and $f(H_2O)$, rather than pressure, as a result of the steep geothermal gradient, which intersects the vertical portion of the amphibole solidus. The abundance of amphibole, combined with relatively small amounts of melting, initially leave some amphibole in the residuum beneath the forearc. As the hydrated peridotite is downdragged to greater temperatures and pres-

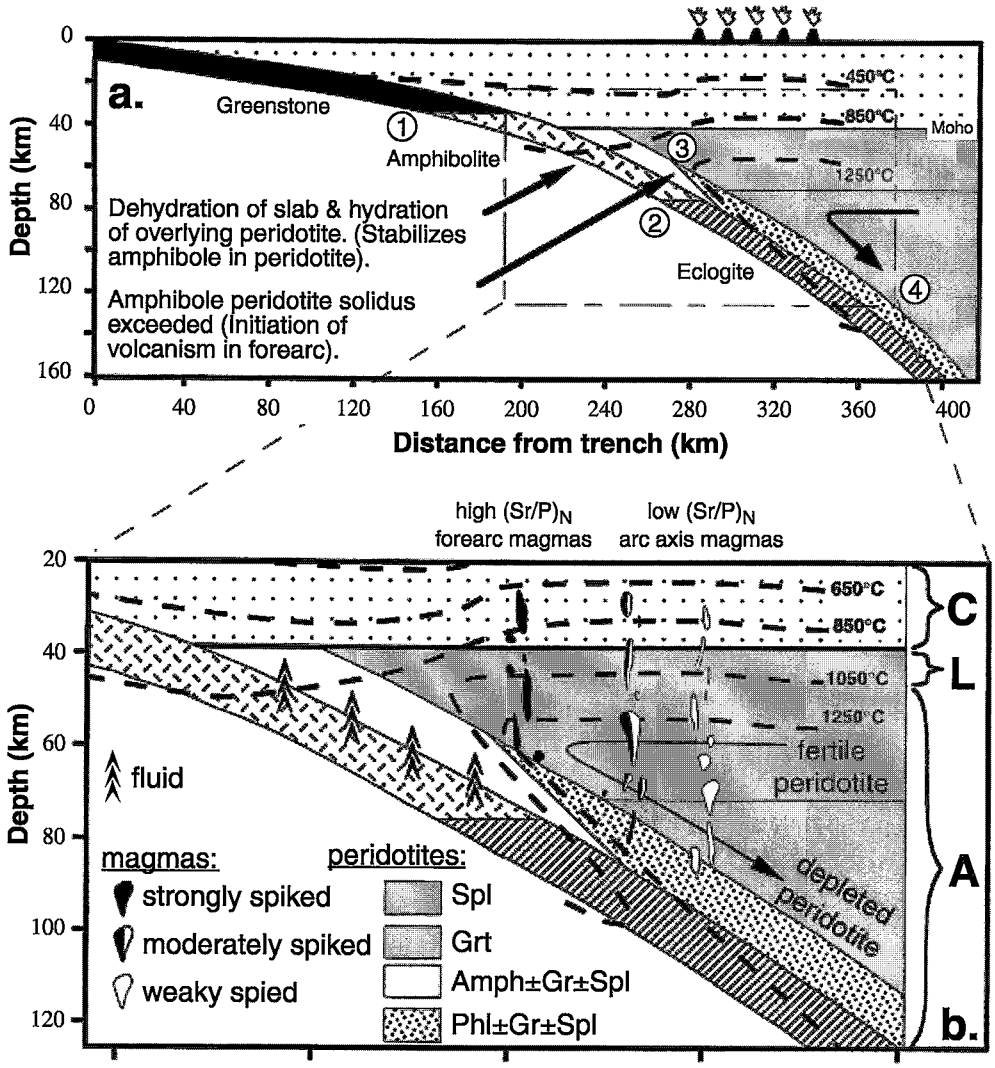

FIG. 10. a. Sketch depicting petrogenesis of the Lassen lavas. Slab dip and Moho from Guffanti *et al.* (1990), and Stanley *et al.* (1990), respectively. Isotherms are estimated based upon thermal models for the top of a young (5 Ma) subducting slab, taken from Peacock (1993). Circles with numbers represent dehydration and melting reactions. Stability fields of epidote in basalt (reaction 1), amphibole in basalt (reaction 2), and amphibole in peridotite (reaction 3) are based upon a compromise among results compiled by Wyllie (1979), Lambert & Wyllie (1972), Green (1973), and BVTP (1981), as suggested by Davies & Stevenson (1992). Phase relations involving phlogopite determined by Sudo & Tatsumi (1990). Dry basalt solidus for top of slab (reaction 4) from Green & Ringwood (1968). b. Detail of Fig. 10a. C is crust, L is lithosphere, and A is asthenosphere. Dehydration of amphibole in the subducting slab hydrates the superjacent mantle to a slab depth of 70 km. The width of the zone of peridotite hydration is assumed to be approximately 10 km. The introduction of fluids to the wedge peridotite stabilizes amphibole and phlogopite, and enriches the wedge in incompatible elements, most notably Sr and Pb. The peridotite is down-dragged beneath the forearc region, where the amphibole peridotite solidus is exceeded at about 1150°C. Melts generated in the presence of amphibole are characterized by depletions in Ta and Nb (as a result of previous enrichment of the wedge in a low-Ta and low-Nb fluid-derived component, and the slightly higher compatibility of Ta and Nb in amphibole compared to other minerals). Progressive dehydration of the amphibole peridotite with depth results in decreasing fluid-contributed signature from west to east across the arc. As a result, lavas erupted along the main axis of the arc lack the Sr spikes and Ta and Nb depletions characteristic of lavas erupted in the forearc region. Initiation of volcanism to the east may result from dehydration of another phase, such as phlogopite, in the hydrated portion of the mantle wedge above the slab. Depleted peridotites may be relatively abundant in the forearc as a result of corner flow in the mantle wedge, which transfers asthenosphere depleted through melt extraction in the back arc and arc axis into the forearc.

sures, and as more melt is extracted from the wedge, the amount of amphibole in the source decreases. This is manifest in a less prominent fluid-contributed geochemical signature in the magmas of the arc axis and backarc. Thus, the Sr spike, as well as the Ta and Nb troughs, steadily decrease away from the trench.

Geochemical and mineralogical evidence suggests that the strongly spiked lavas in the forearc are generated from more depleted mantle than the weakly spiked lavas erupted in the arc axis (see above; Clynne & Borg 1997). The relative abundance of fluid derived from the melting of amphibole beneath the forearc may promote melting of more refractory peridotites, whereas the paucity of water beneath the arc axis may prevent melting of all but the most fertile peridotites. The combined effects of melt extraction and corner flow in the mantle wedge may also promote melting of more depleted mantle in the forearc by producing a greater proportion of depleted peridotite sources in the forearc relative to the backarc. Polybaric extraction of melt in the asthenosphere beneath the backarc and arc axis depletes the peridotites in incompatible elements, and results in more Mg-rich residual phases. Relatively shallow peridotites of the asthenospheric mantle wedge, that have been previously melted, are transferred into the forearc superjacent to the slab, where they may undergo a second stage of melting in the presence of slab-derived fluid (Fig. 10b). In contrast to the forearc, corner flow provides a continuous supply of relatively fertile peridotites to the backarc and arc axis. Thus, peridotite sources beneath the arc axis and backarc may be more fertile, whereas peridotite sources beneath the forearc tend to be more depleted.

There is abundant geochemical evidence that the sub-arc mantle wedge has been enriched through addition of a sediment-like component. The addition of this component is likely to be associated with a previous subduction event because 1) the size of the geochemical signature attributed to sediment is similar in both the strongly and weakly spiked lavas, indicating that the sediment enrichment does not accompany enrichment of modern slab-derived fluids, and 2) Pb isotopic values of the currently subducting sediment (as well as crustal rocks) observed in the region are not sufficiently radiogenic to produce the high $^{207}Pb/^{204}Pb$ observed in the weakly spiked lavas. Old sediments with higher $^{207}Pb/^{204}Pb$ than the modern sediments are, therefore, likely to be the source of the radiogenic Pb isotopic signatures of the weakly spiked lavas.

The origin of the elevated oxygen isotopic values in the Lassen primitive lavas remains an outstanding problem. The analyses were performed on whole-rock powders; no data are available on mineral separates. Although it seems unlikely, it is possible that the groundmasses of these lavas have interacted with meteoric water. Another possibility is that the $\delta^{18}O$ of wedge peridotites have been affected by the addition of slab-derived fluids. Although recent studies show elevated $\delta^{18}O$ in fresh to altered oceanic crust (*e.g.*, Staudigel *et al.* 1995), little is known of the processes of oxygen isotope fractionation in the reactions that produce the slab fluid. Finally, Harmon & Hoefs (1995) have suggested that the oxygen isotopic composition of mantle-derived melts is heterogeneous and may attain values as high as 8. Thus, it is conceivable that the elevated $\delta^{18}O$ of the Lassen primitive lavas is a primary feature of their mantle sources.

Conclusions

The geochemical signatures observed in primitive lavas erupted from small centers across the southernmost Cascade arc are produced by the varied contribution of slab-derived fluids to the mantle wedge, and not by differentiation processes. All lavas have a prominent sediment-contributed geochemical signature, which does not correlate with the modern subduction (fluid-contributed) signature, and is interpreted to reflect enrichment of the mantle wedge in an older subduction regime. Addition of fluid to the mantle wedge beneath the forearc stabilizes amphibole, produces enrichments in unradiogenic Sr and Pb, and depletions in Ta and Nb. High concentrations of Sr and Pb in the fluid allow it to control the Sr and Pb isotopic signatures of magmas derived from fluid-rich sources. The presence of amphibole in the wedge may contribute to the size of the Ta and Nb depletions observed in the lavas as well, because of the greater compatibility of these elements in amphibole relative to other phases likely to be present in the mantle wedge. Progressive dehydration of the mantle wedge with depth results in a smaller fluid-contributed geochemical signature in lavas erupted in the arc axis and back-arc regions. Higher abundances of incompatible elements in magmas derived from fluid-poor sources result from the melting of more fertile mantle, whereas lower abundances of incompatible elements in magmas derived from fluid-rich sources result from the melting of less fertile mantle. Thus, the lavas with a limited fluid-contributed geochemical signature are derived from peridotites that are compositionally similar to an OIB-source, whereas lavas with a more prominent fluid-contributed geochemical signature are derived from peridotites that are more similar to a MORB-source. This study illustrates the profound influence that slab-derived fluids can have on 1) major element, trace element, and isotopic systematics of arc magmas, 2) the modal mineralogy of the source peridotites in the mantle wedge, and 3) the melting processes in the mantle wedge.

Acknowledgements

This manuscript was improved by reviews by J. Brophy, J. Davidson, R. Martin, R. Christiansen, and W. Hildreth. We thank D. Barker, D. Smith, W.

Leeman, M. Cloos, J. Gill, and, P. Muffler for insightful discussions and for providing reviews of earlier versions of the manuscript. We are indebted to P. Bruggman, D. Siems, J. Taggert, and G. Wandless for providing analytical assistance on INAA and XRF analyses. Support was provided by the Geology Foundation of the University of Texas at Austin.

References

Aoki, K. (1971): Petrology of mafic inclusions from Itinomegata, Japan. *Contrib. Mineral. Petrol.* **30**, 314-331.

Arth, J.G. (1976): Behavior of trace elements during magmatic processes – a summary of theoretical models and their application. *J. Res. U.S. Geol. Surv.* **4**, 41-47.

Bacon, C.R. (1990): Calc-alkaline, shoshonitic, and primitive tholeiitic lavas from monogenetic volcanoes near Crater Lake, Oregon. *J. Petrol.* **31**, 135-166.

_____, Bruggman, P.E., Christiansen, R.L., Clynne, M.A., Donnelly-Nolan, J.M. & Hildreth, W. (1997): Primitive magmas at five Cascade volcanoes: melts from hot, heterogeneous sub-arc mantle. *Can. Mineral.* **35**, 397-424.

_____ & Druitt, T.H. (1988): Compositional evolution of the zoned calcalkaline magma chamber of Mount Mazama, Crater Lake, Oregon. *Contrib. Mineral. Petrol.* **98**, 224-256.

Baedecker, R.A. & McKown, D.M. (1987): Instrumental neutron activation analyses of geochemical samples. *U.S. Geol. Surv., Bull.* **1770**, H1-H14.

Bailey, J.C., Frolova, T.I. & Burikova, I.A. (1989): Mineralogy, geochemistry, and petrogenesis of Kurile island-arc basalts. *Contrib. Mineral. Petrol.* **102**, 265-280.

Baker, M.B., Grove, T.L. & Price, R. (1994): Primitive basalts and andesites from Mt. Shasta region, N. California: products of varying melt fraction and water content. *Contrib. Mineral. Petrol.* **118**, 111-129.

Basaltic Volcanism Study Project (1981): *Basaltic Volcanism on the Terrestrial Planets*. Pergamon, New York, N.Y.

Beattie, P. (1993): The generation of uranium series disequilibria by partial melting of spinel peridotite: constraints from partitioning studies. *Earth Planet. Sci. Lett.* **117**, 379-391.

Ben Othman, D. White, W.M. & Patchett, J. (1989): The geochemistry of marine sediments, island arc magma genesis, and crust–mantle recycling. *Earth Planet. Sci. Lett.* **94**, 1-21.

Borg, L.E. (1995): *The Origin and Evolution of Magmas from the Lassen Region of the Southernmost Cascades, California.* Ph.D. dissertation, Univ. of Texas at Austin, Austin, Texas.

_____, Clynne, M.A. & Bullen, T.D. (1994): Influence of the subducting slab on partial melting of wedge peridotites in the generation of calc-alkaline lavas from the southernmost Cascades. *Geol. Soc. Am., Abstr. Programs* **26**, A-331.

_____, _____ & Walker, N.W. (1992): Evidence for multiple sources from isotopic and geochemical variation of lavas across the southernmost Cascade arc, California. *Trans. Am. Geophys. Union* **73**, 646 (abstr.).

Brenan, J.M., Shaw, H.F., Ryerson, F.J. & Phinney, D.L. (1995): Experimental determination of trace-element partitioning between pargasite and a synthetic hydrous andesitic melt. *Earth Planet. Sci. Lett.* **135**, 1-11.

Bullen, T.D. & Clynne, M.A. (1989): Coupled spatial, chemical, and isotopic characteristics of primitive lavas from the Lassen region, California. *In* Continental Magmatism Abstracts. *New Mexico Bur. Mines Mineral Res. Bull.* **131**, 33.

_____ & _____ (1990): Trace element and isotopic constraints on magmatic evolution at Lassen Volcanic Center. *J. Geophys. Res.* **95**, 19671-19691.

Carlson, R.W. & Hart, W.K. (1987): Crustal genesis on the Oregon Plateau. *J. Geophys. Res.* **92**, 6191-6206.

Chen, Chu-Yung & Frey, F.A. (1985): Trace element and isotopic geochemistry of lavas from Haleakala volcano east Maui, Hawaii: implications for the origin of Hawaiian basalts. *J. Geophys. Res.* **90**, 8743-8768.

Church, S.E. (1976): The Cascade Mountains revisited: re-evaluation in light of new lead isotopic data. *Earth Planet. Sci. Lett.* **29**, 175-188.

_____ (1985): Genetic interpretation of lead-isotopic data from the Columbia River basalt group, Oregon, Washington, and Idaho. *Geol. Soc. Am., Bull.* **96**, 676-690.

_____ & Tatsumoto, M. (1975): Lead isotope relations in ocean ridge basalts from the Juan de Fuca – Gorda ridge area, N.E. Pacific Ocean. *Contrib. Mineral. Petrol.* **53**, 253-279.

_____ & Tilton, G.R. (1973): Lead and strontium isotopic studies in the Cascade Mountains: bearing on andesite genesis. *Geol. Soc. Am., Bull.* **84**, 431-454.

Clague, D.A. & Frey, F.A. (1982): Petrology and trace element geochemistry of the Honolulu volcanics, Oahu: implications for the oceanic mantle below Hawaii. *J. Petrol.* **23**, 447-504.

Clynne, M.A. (1990): Stratigraphic, lithologic, and major-element geochemical constraints on magmatic evolution at the Lassen volcanic center, California. *J. Geophys. Res.* **95**, 19651-19669.

_____ (1993): *Geologic Studies of the Lassen Volcanic Center, Cascade Range, California.* Ph.D. dissertation, Univ. of California, Santa Cruz, California.

_____ & Borg, L.E. (1997): The compositions of olivine and chromian spinel in primitive tholeiitic and calc-alkaline

lavas from the southernmost Cascade range: a reflection of source fertility. *Can. Mineral.* **35**, 453-472.

CONNARD, G., COUCH, R., ROY, J., PITTS, G.S. & KULM, S. (1984): Heat flow map of western Oregon and Washington. *In* Atlas of the Ocean Drilling Margin Program, Western Oregon – Washington, Continental Margin and Adjacent Ocean Floor, Region V (L.D. Kulm *et al.*, eds.). Joint Oceanographic Institutions, Inc., Marine Science International, Woods Hole, Massachusetts. Map sheet 6, with text, scale 1:2,000,000.

DAVIDSON, J.P., DUNGAN, M.A., FERGUSON, K.M. & COLUCCI, M.T. (1987): Crust–magma interactions and the evolution of arc magmas: The San Pedro – Pellado volcanic complex, southern Chilean Andes. *Geology* **15**, 443-446.

DAVIES, J.H. & STEVENSON, D.J. (1992): Physical model of source region of subduction zone volcanics. *J. Geophys. Res.* **97**, 2037-2070.

DAVIS, E.E., MOTTL, M.J., FISHER, A.T. *et al.* (1992): Proceedings of the Ocean Drilling Program: Initial Report 139. Ocean Drilling Program, College Station, Texas.

DEPAOLO, D.J. (1981): A neodymium and strontium isotopic study of the Mesozoic calc-alkaline granitic batholiths of the Sierra Nevada and Peninsular ranges, California. *J. Geophys. Res.* **86**, 10470-10488.

_____ (1988): *Neodymium Isotope Geochemistry: an Introduction.* Springer-Verlag, Berlin, Germany.

DEFANT, M.J. & DRUMMOND, M.S. (1990a): Derivation of some modern arc magmas by melting of young subducted lithosphere. *Nature* **347**, 662-665.

_____ & _____ (1990b): Derivation of some modern magmas through melting of young subducted lithosphere. *Trans. Am. Geophys. Union*, **71**, 1715 (abstr.).

DICK, H.J.B. & FISHER, R.L. (1984): Mineralogic studies of the residues of mantle melting: abyssal and alpine-type peridotites. *In* Kimberlites. II. The Mantle and Crust – Mantle Relationships (J. Kornprobst, ed.). Elsevier, Amsterdam, The Netherlands (295-308).

DUNN, T., STOLPER, E.M. & BAKER, M.B. (1993): Partial melting of an amphibole-bearing lherzolite at 1.5 GPa. *Geol. Soc. Am., Abstr. Programs* **25**, A-213.

EABY, J., CLAGUE, D.A. & DELANEY, J.R. (1984): Sr isotopic variations along the Juan de Fuca Ridge. *J. Geophys. Res.* **89**, 7883-7890.

ELLAM, R.M. & HAWKESWORTH, C.J. (1988): Elemental and isotopic variations in subduction related basalts: evidence for a three component model. *Contrib. Mineral. Petrol.* **98**, 72-80.

FREY, F.A. & CLAGUE, D.A. (1983): Geochemistry of diverse basalt types from Loihi seamount, Hawaii: petrogenetic implications. *Earth Planet. Sci. Lett.* **66**, 337-355.

FUJII, T. & SCARFE, C.M. (1985): Composition of liquids coexisting with spinel lherzolite at 10 kbar and the genesis of MORBs. *Contrib. Mineral. Petrol.* **90**, 18-28.

GILL, J.B. (1981): *Orogenic Andesites and Plate Tectonics.* Springer-Verlag, Berlin, Germany.

_____ (1984): Sr–Pb–Nd isotopic evidence that both MORB and OIB sources contribute to oceanic island arc magmas in Fiji. *Earth Planet. Sci. Lett.* **68**, 443-458.

GREEN, D.H. (1973): Contrasted melting relations in a pyrolite upper mantle under mid-oceanic ridge, stable crust, and island arc environments. *Tectonophys.* **17**, 285-297.

_____ & RINGWOOD A.E. (1968): Genesis of the calc-alkaline igneous rock suite. *Contrib. Mineral. Petrol.* **18**, 105-162.

GREEN, T.H., SIE, S.H., RYAN, C.G. & COUSENS, D.R. (1989): Proton microprobe-determined partitioning of Nb, Ta, Zr, Sr, and Y between garnet, clinopyroxene, and basaltic magma at high pressure and temperature. *Chem. Geol.* **74**, 201-206.

GUFFANTI, M., CLYNNE, M.A. & MUFFLER, L.J.P. (1996): Thermal and mass implications of magmatic evolution in the Lassen volcanic region, California, and minimum constraints on basalt influx to the lower crust. *J. Geophys. Res.* **101**, 3001-3013.

_____, _____, SMITH, J.G., MUFFLER, L.J.P. & BULLEN, T.D. (1990): Late Cenozoic volcanism, subduction, and extension in the Lassen region of California, southern Cascade range. *J. Geophys. Res.* **95**, 19453-19464.

_____ & WEAVER, C.S. (1988): Distribution of late Cenozoic volcanic vents in the Cascade Range: volcanic arc segmentation and regional tectonic considerations. *J. Geophys. Res.* **93**, 6513-6529.

HARMON, R.S. & HOEFS, J. (1995): Oxygen isotope heterogeneity of the mantle deduced from global ^{18}O systematics of basalts from different geotectonic settings. *Contrib. Mineral. Petrol.* **120**, 95-114.

HART, S.R. (1984): A large-scale isotope anomaly in the Southern Hemisphere mantle. *Nature* **309**, 753-757.

_____ (1988): Heterogeneous mantle domains: signatures, genesis and mixing chronologies. *Earth Planet. Sci. Lett.* **90**, 273-296.

_____ & BROOKS, C. (1974): Clinopyroxene–matrix partitioning of K, Rb, Cs, Sr, and Ba. *Geochim. Cosmochim. Acta* **38**, 1799-1806.

_____ & DUNN, T. (1993): Experimental cpx/melt partitioning of 24 trace elements. *Contrib. Mineral. Petrol.* **113**, 1-8.

HAWKESWORTH, C.J., HERGT, J.M., ELLAM, R.M. & MCDERMOTT, F. (1991): Element fluxes associated with subduction related magmatism. *Phil. Trans., R. Soc. Lond.* **A335**, 393-405.

HEGNER, E. & TATSUMOTO, M. (1987): Pb, Sr, and Nd isotopes in basalts and sulfides from the Juan de Fuca Ridge. *J. Geophys. Res.* **92**, 11380-11386.

HENDERSON, P. (1982): *Inorganic Geochemistry.* Pergamon Press, Oxford, U.K.

HILDRETH, W. & MOORBATH, S. (1988): Crustal contributions to arc magmatism in the Andes of central Chile. *Contrib. Mineral. Petrol.* **98**, 455-489.

HOFMANN, A.W. (1988): Chemical differentiation of the earth: the relationship between mantle, continental crust, and oceanic crust. *Earth Planet. Sci. Lett.* **90**, 297-314.

_____ & WHITE, W.M. (1983): Ba, Rb, and Cs in the Earth's mantle. *Z. Naturforsch.* **38a**, 256-266.

HUGHES, S.S. (1990): Mafic magmatism and associated tectonism of the Central High Cascade range, Oregon. *J. Geophys. Res.* **95**, 19623-19638.

HYNDMAN, R.D. & WANG, K. (1993): Thermal constraints on the zone of major thrust earthquake failure: the Cascadia subduction zone. *J. Geophys. Res.* **98**, 2039-2060.

IRVINE, T.N. & BARAGAR, W.R.A. (1971): A guide to the chemical classification of the common rocks. *Can. J. Earth Sci.* **8**, 523-548.

JAQUES, A.L. & GREEN, D.H. (1980): Anhydrous melting of peridotite at 0–15 kb pressure and the genesis of tholeiitic basalts. *Contrib. Mineral. Petrol.* **73**, 287-310.

KAY, R.W. (1978): Aleutian magnesian andesites: melts from subducted Pacific ocean crust. *J. Volcanol. Geotherm. Res.* **4**, 117-132.

_____ & KAY, S.M. (1988): Crustal recycling and the Aleutian arc. *Geochim. Cosmochim. Acta* **52**, 1351-1359.

KAY, S.M. & KAY, R.W. (1985): Aleutian tholeiitic and calc-alkaline magma series. I. The mafic phenocrysts. *Contrib. Mineral. Petrol.* **90**, 276-290.

_____, RAMOS, V.A. & MARQUEZ, M. (1991): High Mg dacites (adakites) in Argentina at 48°S associated with slab-melting at 12 Ma prior to the collision of the Chile rises. *Trans. Am. Geophys. Union* **72**, 293 (abstr.).

_____, _____ & _____ (1993): Evidence in Cerro Pampa volcanic rocks for slab-melting prior to ridge–trench collision in southern South America. *J. Geol.* **101**, 703-714.

KLEIN, E.M. & LANGMUIR, C.H. (1987): Global correlations of ocean ridge basalt chemistry with axial depth and crustal thickness. *J. Geophys. Res.* **92**, 8089-8115.

LAMBERT, I.B. & WYLLIE, P.J. (1972): Melting of gabbro (quartz eclogite) with excess water to 35 kilobars, with geological applications. *J. Geol.* **80**, 693-708.

LEEMAN, W.P., SMITH, D.R., HILDRETH, W., PALACZ, Z. & ROGERS, N. (1990): Compositional diversity of Late Cenozoic basalts in a transect across the southern Washington Cascades: implications for subduction zone magmatism. *J. Geophys. Res.* **95**, 19561-19582.

LEMARCHAND, F., VILLEMANT, B. & CALAS, G. (1987): Trace element distribution coefficients in alkaline series. *Geochim. Cosmochim. Acta* **51**, 1071-1081.

LEWIS, T.J., BENTKOWSKI, W.H., DAVIS, E.E., HYNDMAN, R.D., SOUTHER, J.G. & WRIGHT, J.A. (1989): Thermal structure of the northern (Canadian) Cascades. *U.S. Geol. Surv., Open-File Rep.* **89-178**, 104-121.

LUHR, J.F. (1993): Slab-derived fluids and partial melting in subduction zones: insights from two contrasting Mexican volcanoes (Colima and Ceboruco). *J. Volcanol. Geotherm. Res.* **54**, 1-18.

_____ & CARMICHAEL, I.S.E. (1985): Jorullo volcano, Michoacán, Mexico (1759–1754): the earliest stages of fractionation in calc-alkaline magmas. *Contrib. Mineral. Petrol.* **90**, 142-161.

MCBIRNEY, A.R. (1968): Petrochemistry of the Cascade andesite volcanoes. *Oregon Dep. Geol. Mineral. Ind., Bull.* **62**, 101-107.

MCKENZIE, D. & O'NIONS, R.K. (1991): Partial melt distributions from inversion of rare earth element concentrations. *J. Petrol.* **32**, 1021-1091.

MEIJER, A. KWON, T.-T. & TILTON, G.R. (1990): U–Th–Pb partitioning behavior during partial melting in the upper mantle: implications for the origin of high Mu components and the "Pb paradox". *J. Geophys. Res.* **95**, 433-448.

MILLHOLLEN, G.L., IRVING, A.J. & WYLLIE, P.J. (1974): Melting interval of peridotite with 5.7 percent water to 30 kbars. *J. Geol.* **82**, 575-587.

MIYASHIRO, A. (1974): Volcanic rock series in island arcs and active continental margins. *Am. J. Sci.* **274**, 321-355.

MORRIS, J.D., LEEMAN, W.P. & TERA, F. (1990): The subduction component in island arc lavas: constraints from Be isotopes and B–Be systematics. *Nature* **344**, 31-36.

PAWLEY, A.R. & HOLLOWAY, J.R. (1993): Water sources for subduction zone volcanism: new experimental constraints. *Science* **260**, 664-667.

PEACOCK, S.M. (1993): Large-scale hydration of the lithosphere above subducting slabs. *Chem. Geol.* **108**, 49-59.

PLANK, T. & LANGMUIR, C.H. (1988): An evaluation of the global variations in the major element chemistry of arc basalts. *Earth Planet. Sci. Lett.* **90**, 349-370.

RAPP, R.P., WATSON, E.B. & MILLER, C.F. (1991): Partial melting of amphibolite/eclogite and the origin of Archean trondjemites and tonalites. *Precambrian Res.* **51**, 1-25.

RODEN, M.F., FREY, F.A. & CLAGUE, D.A. (1984): Geochemistry of tholeiitic and alkalic lavas from the Koolau range,

Oahu, Hawaii: implications for Hawaiian volcanism. *Earth Planet. Sci. Lett.* **69**, 141-158.

RUSHMER, T. (1991): Partial melting of two amphibolites: contrasting experimental results under fluid absent conditions. *Contrib. Mineral. Petrol.* **107**, 41-59.

SHERROD, D.R. & SMITH, J.G. (1990): Quaternary extrusion rates of the Cascade Range, northwestern United States and southern British Columbia. *J. Geophys. Res.* **95**, 19465-19474.

STANLEY, W.D., MOONEY, W.D. & FUIS, G.S. (1990): Deep crustal structure of the Cascade range and surrounding regions from seismic refraction and magnetotelluric data. *J. Geophys. Res.* **95**, 19419-19438.

STAUDIGEL, H., DAVIES, G.R., HART, S.R., MARCHANT, K.M. & SMITH, B.M. (1995): Large scale isotopic Sr, Nd and O isotopic anatomy of altered oceanic crust: DSDP/ODP sites 417/418. *Earth Planet. Sci. Lett.* **130**, 169-185.

STERN, C.R., FUTA, K. & MUEHLENBACHS, K. (1984): Isotope and trace element data for orogenic andesites from the Austral Andes. *In* Andean Magmatism: Chemical and Isotopic Constraints (R.S. Harmon & B.A. Barreiro, eds.). Shiva, Cheshire, U.K. (31-47).

STOLPER, E. & NEWMAN, S. (1994): The role of water in the petrogenesis of Mariana trough magmas. *Earth Planet. Sci. Lett.* **121**, 293-325.

SUDO, A. & TATSUMI, Y. (1990): Phlogopite and K-amphibole in the upper mantle: implications for magma genesis in subduction zones. *Geophys. Res. Lett.* **17**, 29-32.

SUN, SHEN-SU & MCDONOUGH, W.F. (1989): Chemical and isotopic systematics of oceanic basalts: implications for mantle composition and processes. *In* Magmatism in the Ocean Basins (A.D. Saunders & M.J. Norry, eds.). Blackwell Scientific Publ., London, U.K. (313-345).

TAKAHASHI, E. (1980): Thermal history of lherzolite xenoliths. I. Petrology of lherzolite xenoliths from the Ichinomegata crater, Oga Peninsula, northeast Japan. *Geochim. Cosmochim. Acta* **44**, 1643-1658.

_____ (1986): Genesis of calc-alkaline andesite magma in a hydrous mantle–crust boundary: petrology of lherzolite xenoliths from the Ichinomegata crater, Oga Peninsula, northeast Japan. II. *J. Volcanol. Geotherm. Res.* **29**, 355-395.

TATSUMI, Y. (1986): Formation of the volcanic front in subduction zones. *Geophys. Res. Lett.* **13**, 717-720.

_____ (1989): Migration of fluid phases and genesis of basalt magmas in subduction zones. *J. Geophys. Res.* **94**, 4697-4707.

_____ & ISHIZAKA, K. (1982): Magnesian andesite and basalt from Shodo-Shima island, southwest Japan, and their bearing on the genesis of calc-alkaline andesites. *Lithos* **15**, 161-172.

TATSUMOTO, M., HEGNER, E. & UNRUH, D.M. (1987): Origin of the west Maui volcanic rocks inferred from Pb, Sr, and Nd isotopes and a multicomponent model for ocean basalts. *U.S. Geol. Surv., Prof. Pap.* **1350**, 723-744.

THOMPSON, R.N., MORRISON, M.A., HENDRY, G.L. & PARRY, S.J. (1984): An assessment of the relative roles of a crust and mantle in magma genesis: an elemental approach. *Phil. Trans., R. Soc. Lond.* **A310**, 549-590.

TILLING, R.I., WRIGHT, T.L. & MILLARD, H.T., JR. (1987): Trace-element chemistry of Kilauea and Mauna Loa lava in space and time; a reconnaissance. *U.S. Geol. Surv., Prof. Pap.* **1350**, 641-689.

WHITE, W.M., HOFMANN, A.W. & PUCHELT, H. (1987): Isotope geochemistry of Pacific mid-ocean ridge basalt. *J. Geophys. Res.* **92**, 4881-4893.

WILSON, M. (1989): *Igneous Petrogenesis.* Unwin Hyman Ltd., London, U.K.

WITT-EICKSCHEN, G. & HARTE, B. (1994): Distribution of trace elements between amphibole and clinopyroxene from mantle peridotites of the Eifel (western Germany): an ion-microprobe study. *Chem. Geol.* **117**, 235-250.

WYLLIE, P.J. (1979): Magmas and volatile components. *Am. Mineral.* **64**, 469-500.

YOGODZINSKI, G.M., VOLYNETS, O.N., KOLOSKOV, A.V., SELIVERSTOV, N.I. & MATVENKOV, V.V. (1994): Magnesian andesites and the subduction component in a strongly calc-alkaline series at Piip volcano, far western Aleutians. *J. Petrol.* **35**, 163-204.

ZINDLER, A. & HART, S.R. (1986): Chemical geodynamics. *Annu. Rev. Earth Planet. Sci.* **14**, 493-571.

Received November 8, 1995, revised manuscript accepted November 8, 1996.